Inclusive lepton pair production through virtual W, Z and gauge bosons in proton-antiproton collisions

Autor(en): **Greub, C. / Bettems, J.M. / Minkowski, P.**

Objekttyp: **Article**

Zeitschrift: **Helvetica Physica Acta**

Band (Jahr): **64 (1991)**

Heft 8

PDF erstellt am: **27.04.2024**

Persistenter Link: https://doi.org/10.5169/seals-116342

Helvetica Physica Acta
Vol. 64 (1991)

0018-0238/91/081277-63$1.50+0.20/0

Inclusive Lepton Pair Production through Virtual W,Z and γ Gauge Bosons in Proton-Antiproton Collisions *

C. Greub
Deutsches Elektronen Synchroton DESY
Notkestrasse 85, D-2 Hamburg, Germany

J.M. Bettems, P. Minkowski
Institute for Theoretical Physics
University of Bern
Sidlerstr. 5, CH-3012 Bern, Switzerland

October 1991

(16. V. 1991, revised 31. X. 1991)

Abstract

Production cross sections for the inclusive reactions

$$p + \bar{p} \to \left\{ \begin{array}{lll} W^{\mp} & + & X_W \\ Z,\gamma & + & X_{Z,\gamma} \end{array} \right\} \to \left\{ \begin{array}{lllll} e^{\mp} & + & \overset{(-)}{\nu} & + & X_W \\ e^- & + & e^+ & + & X_{Z,\gamma} \end{array} \right\}$$

$$p_1 + p_2 \to q + p_X \to l_1 + l_2 + p_X$$

are calculated in differential and integrated form. The cross sections depend on five independent final state lepton momentum variables and parametrically on the individual quark - gluon momentum fractions of the incident hadrons and on their center of mass energy ($\sqrt{s}$). Hard processes are calculated through first order in the strong coupling constant, the scale being set by the transverse momentum of the lepton pair ($q_\perp$). A Sudakov exponentiation independent of $\sqrt{s}$ is shown to extend smoothly from small $q_\perp$ into the hard scattering domain. Numerical results for $\sqrt{s}$ = .63 and 1.8 TeV are presented.

*Work supported in part by Schweizerischer Nationalfonds

Contents

1 Introduction and outline

In this paper a systematic analysis of lepton pair production through virtual gauge bosons ($W^{\pm}$, Z , γ) in proton - antiproton collisions is presented.
Many aspects of Drell-Yan processes have been originally studied in the perturbative region [1] . The evolution of parton densities [2] was related to a systematic expansion in the strong coupling constant on the level of the associated parton subprocesses [3] . More recently detailed numerical studies have been carried out [4] , also calculations complete to second order in α_s have been presented [5] , pertaining to this region.
The Sudakov region was systematically studied within QCD, for purely hadronic processes by Dokshitzer, Dyakonov and Troyan [6] . The extension of the Sudakov exponentiation to the Sudakov region as appropriate for Drell - Yan processes, in particular the transformation to impact parameter space, was discussed by Soper and Collins [7] .

The synthesis of regularizing parton densities in a way consistent with the Sudakov

form factor for Drell - Yan processes, to first subleading order in QCD, was achieved by Altarelli, R. K. Ellis, Greco and Martinelli [8] , and applied to subsequent numerical calculations of W - and Z - production cross sections [9] .

Direct calculations of transverse lepton momentum distributions, complete to next to leading order, have been performed by Aurenche and Lindfors [1] and recently extended by Baer and Reno [10]. We compare our distributions with the ones presented in these papers in the section containing numerical results (figures 7a and 7b) .
We propose to extend all previous analyses in one central aspect : physical inclusive production cross sections of virtual gauge bosons from hadron collisions are calculated in fully differential form with respect to all variables, including hadron and lepton polarizations , which are defined independently from quark gluon subprocess variables. QCD corrections are understood to be performed on this level. Quark gluon subprocesses are calculated and processed in parallel. Partially integrated subprocess cross sections are explicitely compared with actual integrals over the so constructed fully differential cross sections. This comparison allows to kinematically extend complementary approximations: the Sudakov exponentiation, valid for small transverse gauge boson momenta (Sudakov region) , into the perturbative region and perturbative calculations, limited in this paper to first order in α_s , valid for large transverse momenta towards the Sudakov region . This applies to total production cross sections [5] , as well as to to the distributions projected on the transverse momentum or transverse mass of one of the leptons (Jacobian peak) [1] , [10] .

The paper is structured in view of implementing the above strategy : In section 1 the kinematic variables and the dimensional regularization procedure including the interaction of color octet pseudoscalar gluons with quarks are specified. A preview of our results with respect to the Sudakov region and the associated factorization of leptonic variables is given. Detailed derivations are presented in section 2. In section 3 numerical results are presented. Computational details concerning fast algorithms for elliptic integrals and Bessel transforms are described.

1.1 Kinematics of Drell - Yan processes , extension to $4 + 2\varepsilon$ dimensions

The momenta determining the above cross sections are as indicated in the abstract. The relevant kinematic regions are characterized by

a) the (5) final state lepton momentum variables, which we consider measurable in principle :

$$1 : l_{1T}, y_1, l_{2T}, y_2, \varphi(\vec{l}_{1T}, \vec{l}_{2T})$$
or equivalently (1)
$$2 : q^2, q_T, y_q, l_{1T}, \varphi(\vec{q}_T, \vec{l}_{1T})$$

The kinematics in eq. (1) is understood in the center of mass of the incident hadron system, with the z axis of momenta along the proton beam direction. The overall azimutal angle of the two lepton momenta $\vec{l}_{1,2}$ is redundant.

Four momenta are considered in the associated light cone basis :

$$\begin{aligned} v &= (v^+, v^-, \vec{v}_T) \\ v^\pm &= v^0 \pm v^{(z)} \quad ; \quad v^2 = v^+ v^- - v_T^2 \\ v_T^2 &= (\vec{v}_T)^2 \quad ; \quad \mu_T(v)^2 = v^2 + v_T^2 \\ v^\pm &= \mu_T(v) \exp(\pm y_v) \quad ; \quad v^2 / v^1 = \tan(\varphi_v) \end{aligned} \tag{2}$$

Making use of the above azimutal angle redundancy we can set $\varphi_{l_1} = 0$ without loss of generality.

In eq. (2) $\mu_T(v)$, y_v, φ_v denote transverse mass, rapidity and azimutal angle respectively, pertaining to the four momentum v .

We work throughout to lowest order in the electroweak coupling constants. Thus neglecting electroweak radiative corrections, it follows :

$$q = l_1 + l_2 \quad ; \quad \varphi_q = \varphi(\vec{q}_T, \vec{l}_{1T}) \tag{3}$$

Having so defined the final state kinematics and using the second set of independent variables in eq. (1) differential cross sections will be of the form :

$$
\begin{aligned}
& d\sigma = d\Omega_f D \quad ; \quad d\Omega_f = d^4 q \; d l_{1T} \\
& d^4 q = dq^2 \; dq_T^2 \; dy_q \; d\omega_1(\varphi_q)(\pi/2) \\
& d\omega_1(\varphi) = d\varphi/(2\pi) \quad ; \quad \varphi_q \to \varphi
\end{aligned}
\tag{4}
$$

In eq. (4) D describes the differential distribution; the volume elements $d^4 q$, $d\omega_1(\varphi)$ easily generalize to arbitrary dimensions, which we will exploit as infrared regularisation of underlying quark gluon processes :

$$
\begin{aligned}
& d = 4 \to d = 4 + 2\varepsilon \quad ; \quad d^4 q \to d^{4+2\varepsilon} q \\
& d^{4+2\varepsilon} q = dq^2 \; dq_T^2 \; (q_T)^{2\varepsilon} \; dy_q \; d\omega_{1+2\varepsilon}(\underline{\varphi}) \; \pi^{1+\varepsilon}/(2\Gamma(1+\varepsilon)) \\
& d = 4 + 2\varepsilon \to \underline{\varphi} = (\varphi_1, \cdots, \varphi_{1+2\varepsilon})
\end{aligned}
\tag{5}
$$

In eq. (5) $\underline{\varphi}$ denotes the $1 + 2\varepsilon$ angular variables parametrizing the transverse sphere $S_{1+2\varepsilon}$, with volume element $d\omega_{1+2\varepsilon}(\underline{\varphi})$ normalized such that

$$
\int d\omega_{1+2\varepsilon} = 1 \tag{6}
$$

The kinematic regions are further characterized by

b) initial state parameters upon reduction of the processes outlined in the abstract to the subprocess level of quarks, antiquarks, gluons and leptons

$$
\begin{array}{ccccccccccccc}
h_\alpha & + & h_\beta & \to & \left\{ \begin{array}{c} W^\mp \\ Z,\gamma \end{array} \right. & + & \left. \begin{array}{c} X^{W}_{\alpha\beta} \\ X^{Z,\gamma}_{\alpha\beta} \end{array} \right\} & \to & \left\{ \begin{array}{c} e^\mp \\ e^- \end{array} \right. & + & \left. \begin{array}{c} \overset{(-)}{\nu} \\ e^+ \end{array} \right. & + & \left. \begin{array}{c} X^{W}_{\alpha\beta} \\ X^{Z,\gamma}_{\alpha\beta} \end{array} \right\} \\
x_1 p_1 & + & x_2 p_2 & \to & q & + & \hat{p}_X & \to & l_1 & + & l_2 & + & \hat{p}_X
\end{array}
\tag{7}
$$

In eq. (7) h_α stands for quark or antiquark flavors $\overset{(-)}{u}$, $\overset{(-)}{d}$, $\overset{(-)}{c}$, $\overset{(-)}{s}$, $\overset{(-)}{b}$ and gluons g respectively, including helicity quantum numbers. A given subprocess in eq. (7) , denoted $R\,{}^{B}_{\alpha\beta}{}^{X}$ in the following, is thus defined by

$$\begin{aligned} & h_\alpha\,,\ h_\beta\,;\ l_1\,,\ l_2 \text{ and } X\,{}^{B}_{\alpha\beta} \quad ; \quad B = W^{\mp}\,,\ Z\,,\ \gamma \text{ e. g. :} \\ & d + \bar{u} \rightarrow e^- + \bar{\nu} + (n)\,g \quad ; \quad n = 0\,,\ 1\,,\ 2\,\cdots \end{aligned} \tag{8}$$

A complete list and analysis of the reactions $R = R\,{}^{B}_{\alpha\beta}{}^{X}$ is deferred to section 2. Subprocesses involving the top quark are neglected throughout. The corresponding cross sections are too small, to be of numerical interest, even though they do not vanish. In their analysis the top quark mass cannot be neglected. The masses of the remaining partons h_α and leptons are set to zero.

The initial state kinematics is determined by the momentum fractions x_1 , x_2 of respective partons h_α , h_β and the associated subprocess square energy $\hat{s} = x_1\,x_2\,s$.

With the momentum kinematics thus specified, a given subprocess reaction in eq. (7) further depends on the polarization state of individual incoming and outgoing quanta, which we characterize by the respective helicities, extended to $4 + 2\,\varepsilon$ dimensions. Fermion spinors, for a lightlike momentum rotated into the (physical) first four directions, factorize in accordance with the associated Dirac - Clifford algebra :

$$\begin{aligned} & \gamma_A = \gamma_\mu \otimes \mathbf{1}\,(2^\varepsilon \times 2^\varepsilon) \quad ; \quad A = \mu = 0\,,\cdots 3 \\ & \gamma_A = i\,\gamma_5 \otimes \Gamma_a \quad ; \quad A - 3 = a = 1\,,\cdots 2\,\varepsilon \\ & \{\Gamma_a\,,\ \Gamma_b\} = 2\,\delta_{ab}\,\mathbf{1}\,(2^\varepsilon \times 2^\varepsilon) \quad ; \quad a\,,\ b = 1\,,\cdots 2\,\varepsilon \\ & W_{\mathcal{A}\,\mathcal{B}}\,(p\,,\ s\,,\ r) = w_{\mathcal{A}}\,(p\,,\ s)\,v_{\mathcal{B}}\,(r) \\ & \mathcal{A} = 1\,,\cdots 4 \quad ; \quad \mathcal{B} = 1\,,\cdots (2)^\varepsilon \quad ; \quad r = 1\,,\cdots (2)^\varepsilon \end{aligned} \tag{9}$$

In eq. (9) $W_{\mathcal{A}\,\mathcal{B}}$ denotes the full spinor in $4 + 2\,\varepsilon$ dimensions with

$$tr\ \mathbf{1}\,(2^{2+\varepsilon} \times 2^{2+\varepsilon}) = 4\,(2^\varepsilon) \tag{10}$$

For external momenta p, with vanishing components in the extra dimensions :

$$\begin{aligned} p &= (p^+ , p^- , \vec{p}_T) \\ \vec{p}_T &= (p^1 , p^2 , 0 , \cdots 0) \end{aligned} \tag{11}$$

the factorization property shown in eq. (9) reduces the spinor W to the four dimensional spinor w multiplied by the spinor v describing redundant spin components referring to the extra dimensions :

$$\begin{aligned} \frac{1 + \gamma_5}{2} \, w_{\mathcal{A}} (p , s) &\rightarrow \begin{cases} p^{\dot\beta} & ; \quad s = - \quad , \dot\beta = 1 , 2 \\ 0 & ; \quad s = + \end{cases} \\ \frac{1 - \gamma_5}{2} \, w_{\mathcal{A}} (p , s) &\rightarrow \begin{cases} p_\alpha & ; \quad s = + \quad , \alpha = 1 , 2 \\ 0 & ; \quad s = - \end{cases} \end{aligned} \tag{12}$$

In eq. (12) $s = \pm$ denotes positive and negative helicity respectively. For lightlike momenta p, chirality and helicity coincide and the corresponding righthanded (p_α) and lefthanded ($p^{\dot\beta}$) , (complex) spinors are directly labelled by the associated momentum for brevity of notation. The relativistic normalizations are :

$$\begin{aligned} p_\alpha p^*_{\dot\beta} &= p_{\alpha\dot\beta} = (p^0 + \vec{p}\,\vec{\sigma})_{\alpha\dot\beta} \\ | p^\alpha p'_\alpha |^2 &= | p^{\dot\beta} p'_{\dot\beta} |^2 = 2 p p' \end{aligned} \tag{13}$$

In eq. (13) standard (four dimensional) spinor notation is used. The second relation in eq. (13) provides a powerful tool, which we use systematically to calculate spin dependent cross sections.

The redundant fermion spin components

$$v_{\mathcal{B}} (r) \quad ; \quad \mathcal{B} , r = 1 , \cdots , (2)^\varepsilon \text{ with the normalization : } \sum v^*_{\mathcal{B}} \, v_{\mathcal{B}} = 1 \tag{14}$$

can be completely eliminated to all orders in a perturbative expansion from external states and within loops, reducing the trace normalization in eq. (10) to four dimensions :

$$\begin{aligned} & tr\ \mathbf{1}\ (\ 2^{\,2+\varepsilon} \times 2^{\,2+\varepsilon}\ ) \ =\ 4\ (\ 2^{\,\varepsilon}\ ) \quad \rightarrow \\ & tr\ \mathbf{1} \ =\ 4 \end{aligned} \tag{15}$$

keeping external phase space and loop momentum space in $4 + 2\varepsilon$ dimensions. Gauge boson couplings and external polarisation vectors extend to components which are (relatively) pseudoscalar in four dimensional terms, as implied by the factorized form of the γ algebra in eq. (9) . These extended couplings, whence combined with the couplings of W and Z bosons, generate nontrivial parity violating effects in higher orders with respect to the elctroweak interactions. In the approximation adopted in this work these questions can be omitted.
Ultraviolet regularization and subsequent renormalization is understood to be completed prior to infrared (dimensional) regularization.

1.2 Perturbative expansions within QCD

The relatively pseudoscalar QCD couplings are equivalent to introducing besides the color octet vector gluon fields $g_{\mu}^{\,a}$; $a = 1, \cdots, 8$ a set of color octet pseudoscalar gluon fields $\tilde{g}_{\alpha}^{\,a}$; $\alpha = 1, \cdots, 2\varepsilon$ with pseudoscalar coupling to quarks [1] :

$$\begin{aligned} & \mathcal{H}_1 \ =\ \tilde{g}_{s\,\varepsilon}\ \bar{q}\ \Big\{\ \gamma^{\mu}\, g_{\mu} \ +\ i\,\gamma_5 \sum_{\alpha=1}^{2\varepsilon} \tilde{g}_{\alpha}\ \Big\}\ q \\ & g_{\mu} \ =\ g_{\mu}^{\,a}\ (\ \chi_a\ /\ 2\ ) \quad , \quad \tilde{g}_{\alpha} \ =\ \tilde{g}_{\alpha}^{\,a}\ (\ \chi_a\ /\ 2\ ) \end{aligned} \tag{16}$$

The strong coupling constant, $\tilde{g}_{s\,\varepsilon}$ in $4 + 2\varepsilon$ dimensions has the dimension of (mass)$^{-\varepsilon}$:

$$\begin{aligned} & \tilde{g}_{s\,\varepsilon} \ =\ g_{\mu} \left(\frac{4\,\pi}{\mu^{\,2}\ \exp\ (\ \gamma_E\ )} \right)^{\varepsilon\ /\ 2} \\ & \gamma_E \ :\quad \text{Eulers constant} \quad (\ =\ 0.5772\cdots\ ) \end{aligned} \tag{17}$$

Eq. (17) defines the dimensionless renormalized) coupling constant g_{μ} corresponding to the $\overline{MS}$ ultraviolet regularization scheme.

[1] We propose pseudoscalar gluon interactions as a powerful regularization scheme, especially suited to include polarization effects [11] , [12] .

The subprocess cross sections in eq. (7) can be systematically expanded in powers of $(g_\mu)^2$ or equivalently in powers of the rationalized coupling constant

$$\kappa_\mu = \frac{(g_\mu)^2}{16 \pi^2} = \alpha_{s\mu} / (4 \pi) \tag{18}$$

This perturbative expansion is understood in its own right, irrespective of whether specific orders generate an actual approximation to the corresponding physical cross sections.

We have verified the correct structure of the pseudoscalar interactions as given in eq. (18) , through first order with respect to κ_μ .

Physical quantities are renormalization group invariant, i. e. functionals of the running coupling constant κ_μ , obtained in a definite renormalization scheme ($\overline{MS}$ here) :

$$\begin{aligned} &\kappa_\mu = \kappa (r) \quad ; \quad r = (\mu / \Lambda_{\overline{MS}})^2 \\ &r \, \partial_r \kappa = \beta (\kappa) \quad ; \quad -\beta = \kappa^2 \sum_{n=0}^{\infty} b_n \, \kappa^n \\ &b_0 = 11 - (2 / 3) N_{fl} \quad ; \quad b_1 = 102 - (38 / 3) N_{fl} \, ; \cdots \end{aligned} \tag{19}$$

The region where, upon the substitution $\mu \rightarrow q_T$, the perturbative expansion does approximate the physical cross sections, is determined by the three variables $\sqrt{s}$, $q = \sqrt{q^2}$ and q_T . In the following we characterize the perturbative and nonperturbative (Sudakov) regions by :

$$\begin{aligned} &\text{perturbative region :} \quad q \, , \, q_T \gg \Lambda_{\overline{MS}} \\ &\text{Sudakov region :} \quad 0 \leq q_T \ll M = q \quad ; \quad M \gg \Lambda_{\overline{MS}} \end{aligned} \tag{20}$$

The definition of the two regions in eq. (20) includes the overall condition $q \gg \Lambda_{\overline{MS}}$. For the production of real photons at large p_T the condition

$M = q$ can be relaxed. The perturbative region exists also for $q \to 0$, provided $M \gg \Lambda_{\overline{MS}}$.
The range of q values considered here is

$$\begin{aligned} &\text{for } \sqrt{s} = 0.63\ TeV : \quad 20\ GeV \leq q \leq 140\ GeV \\ &\text{for } \sqrt{s} = 1.8\ TeV : \quad 50\ GeV \leq q \leq 140\ GeV \end{aligned} \tag{21}$$

Subprocess cross section are calculated up to first order with respect to κ_μ . A given reaction $R^{B}_{\alpha\beta}{}^{X}$ in eqs. (7 , 8) , involving the (polarized) partons h_α , h_β , contributes to the corresponding $p\,\bar{p}$ process with the initial state flux factor

$$\begin{aligned} d\,\Omega_{i\,\alpha\,\beta} &= d\,x_1\,d\,x_2\,H_{\alpha\,\beta}\,(\,x_1\,,\,x_2\,;\,scale\,) \\ H_{\alpha\,\beta}\,(\,x_1\,,\,x_2\,;\,scale\,) &= h_\alpha\,(\,x_1\,;\,scale\,)\,h_\beta\,(\,x_2\,;\,scale\,) \end{aligned} \tag{22}$$

All calculation are done retaining arbitrary polarization states for the incoming hadrons. The numerical results presented in section 3 are restricted to unpolarized p , $\bar{p}$ scattering.
For the unpolarized case $h_\alpha\,(\,x_1\,;\,scale\,)$ in eq. (22) denotes the spin averaged, scale dependent density of parton h_α with momentum fraction x_1 in the proton. h_β and x_2 refer to the antiproton.

1.3 Structure of the Sudakov cross section [2]

In the Sudakov region, a universal Sudakov form factor is induced in impact parameter space, upon a Fourier - Bessel transformation. Its structure is determined by the dominant infrared properties of the underlying subprocesses, in conjunction with well defined corrections. The expressions involving the Sudakov form factor dominate the physical cross sections. Details of the exponentiation procedure are discussed in section 1.5 . We denote by $d\,\sigma^{S}$ the corresponding contribution to the respective cross sections.

[2] This section is a preview. Details of our approach are described in sections 1.5 and 2.3 [11] .

$d\sigma^S$ contains the following characteristic expressions [11], upon the differential substitutions :

$$\frac{d\sigma^S_{\alpha\beta}}{dq^2\, dq_T^2\, d\bar{\varphi}_q\, dy_q\, dl_{1T}} = X^S_{\alpha\beta}(\underline{q}, l_{1T}, s)$$

$$X^S_{\alpha\beta} = \int d\Omega(l_1')\, q^2\, \delta\left[(q - l_1')^2\right]\, \delta(l_{1T}' - l_{1T})\, Y^S_{\alpha\beta}$$

$$d\Omega(l) = \frac{1}{16\pi}\, dl_T^2\, dy_l \quad , \quad \bar{\varphi}_q = \varphi_q / (2\pi) \tag{23}$$

$$Y^S_{\alpha\beta} = \frac{1}{3s}\, \vartheta_{ph}\, Z^S_{\alpha\beta} \quad , \quad dim(Z^S_{\alpha\beta}) = [m]^{-6}$$

In eq. (23) $\underline{q}$ denotes the full four momentum q , and ϑ_{ph} the characteristic function of physical momenta q , for given $\sqrt{s}$ ($\gg m_p$) :

$$0 \leq q \leq \sqrt{s}$$

$$1 \leq \cosh y_q \leq \frac{s + q^2}{2\sqrt{s}\,\mu_T(q)} \quad ; \quad \mu_T(q) = (q^2 + q_T^2)^{1/2} \tag{24}$$

ϑ_{ph} is factored out from the definition of $Z^S_{\alpha\beta}$ in eq. (23) .

Upon the substitutions in eqs. (23 , 24) the expression for $Z^S_{\alpha\beta}$ becomes :

$$Z^S_{\alpha\beta}(\underline{q}, l_1, l_2, s) = \frac{1}{2}\int_0^\infty b\, db\, \zeta^S_{\alpha\beta}\, J_0(q_T b) \tag{25}$$

$$\zeta^S_{\alpha\beta} = \zeta^S_{\alpha\beta}(b; \underline{q}, l_{1T}, y_{l_1}, s)$$

The quantity $\zeta^S_{\alpha\beta}$ in eq. (25) , i. e. the (differential) Sudakov cross section in impact parameter space , exhibits the s and subprocess independent Sudakov form factor :

$$\zeta^{S}_{\alpha\beta} = \exp\left[S(b, q) \right] \eta^{S}_{\alpha\beta}$$

$$\eta^{S}_{\alpha\beta} = \eta^{S}_{\alpha\beta}(b; \underline{q}, l_{1T}, y_{l_1}, s)$$

$$S(b, q) = \frac{8}{3} \int_0^{\infty} \frac{dq_T^2}{q_T^2} \kappa(q_T) \left[2 \log\left(\frac{q^2}{q_T^2} \right) - 3 \right] J(b, q_T, q)$$

$$J(b, q_T, q) = \begin{cases} J_0(q_T b) - 1 & ; \quad q_T \leq q \\ J_0(q_T b) & ; \quad q_T > q \end{cases} \tag{26}$$

The specific form of the Sudakov form factor as exhibited in eq. (26) is derived in sections 1.5 and 2.3 .
The quantity $\eta^{S}_{\alpha\beta}$ in eq. (26) exhibits the factorization into lepton momentum factor, gauge boson propagator and electroweak couplings, according to the four virtual gauge boson channels in the reactions specified in the abstract :

$$\eta^{S}_{\alpha\beta} = \eta_{\alpha\beta}\left[B, Q(\bar{Q}) \right] \quad ; \quad B = W^{\mp}, Z\gamma$$

$$\eta_{\alpha\beta}\left[B, Q(\bar{Q}) \right] = \begin{cases} \eta_{\alpha\beta}\left[W^{-}, Q(\bar{Q}) \right] & \begin{cases} Q : \alpha\beta = \underline{d}\,\underline{\bar{u}} \\ \bar{Q} : \alpha\beta = \underline{\bar{u}}\,\underline{d} \end{cases} \quad \text{for } W^{-} \\ \eta_{\alpha\beta}\left[W^{+}, Q(\bar{Q}) \right] & \begin{cases} Q : \alpha\beta = \underline{u}\,\underline{\bar{d}} \\ \bar{Q} : \alpha\beta = \underline{\bar{d}}\,\underline{u} \end{cases} \quad \text{for } W^{+} \\ \eta_{\alpha\beta}\left[Z\gamma, Q(\bar{Q}) \right] & \begin{cases} Q : \alpha\beta = \underline{Q}\,\underline{\bar{Q}} \\ \bar{Q} : \alpha\beta = \underline{\bar{Q}}\,\underline{Q} \\ \underline{Q} = \underline{u}, \underline{d} \end{cases} \quad \text{for } Z, \end{cases} \tag{27}$$

In eq. (27) the label Q denotes the subprocesses with a quark out of the proton and an antiquark out of the antiproton. $\bar{Q}$ refers to the subprocesses with an antiquark out of the proton and a quark out of the antiproton. No other initial

state subprocesses contribute to the Sudakov cross section (eq. (23)) to the relevant orders considered.

$\underline{Q}$ is representative for all quark flavors : $\underline{d} = d , s , b$, $\underline{u} = u , c , t$.

As stated above, all subprocesses involving the (anti) top flavor either in the initial or final state are neglected.

The quantities $\eta_{\alpha\beta} \left[B , Q (\bar{Q}) \right]$ in eq. (27) exhibit the factorization into lepton variables - gauge boson propagator - quark variables :

$$\eta_{\alpha\beta} \left[B , Q (\bar{Q}) \right] =$$

$$K_{\alpha\beta} \left[B , Q (\bar{Q}) ; \underline{q} , l_{1T} , y_{l_1} \right] \tilde{H}_{\alpha\beta} \left[Q (\bar{Q}) ; x_1^0 , x_2^0 ; scale = b_0 / b \right]$$

$$b_0 = 2 \exp (- \gamma_E)$$

$$x_1^0 = q \exp (y_q) / \sqrt{s} \quad ; \quad x_2^0 = q \exp (- y_q) / \sqrt{s} \tag{28}$$

In eq. (28) the quantity K, called leptonic factor in the following, contains the electroweak fermion couplings and the gauge boson propagators but does not depend on the impact parameter b. The explicit form of K and its dependence on the specific lepton channel, is given in section 1.6 (eqs. (53 - 61)) .
$\tilde{H}$ depends in a process specific way on the respective (anti) quark densities of the incoming hadrons, evaluated at the momentum scale b_0 / b :

$$\tilde{H}_{\alpha\beta} =$$

$$\begin{cases} \sigma^p (Q_\alpha ; x_1^0 ; b_0 / b) \; \sigma^{\bar{p}} (\bar{Q}_\beta ; x_2^0 ; b_0 / b) & for \; Q \\ \sigma^p (\bar{Q}_\alpha ; x_1^0 ; b_0 / b) \; \sigma^{\bar{p}} (Q_\beta ; x_2^0 ; b_0 / b) & for \; \bar{Q} \end{cases} \tag{29}$$

modulo weak mixing angles

We distinguish here the process specific quark and gluon structure functions

$$\sigma^p (Q , \bar{Q}) \quad , \quad \sigma^{\bar{p}} (Q , \bar{Q})$$

as they appear in eq. (29) from universal but scheme dependent parton densities

$$h^H = Q^H , \bar{Q}^H , g^H$$

The minimally (infrared) subtracted parton densities $(h^{ms})^{H}$; $h = Q , \bar{Q} , g$ of a given hadron H are defined in the next section, where the relation between parton densities $(h^{ms})^{H}$ and process dependent structure functions $\sigma^{H \mid DY , \cdots} (h)$ is also outlined (eqs. (30) - (40)) .
The decomposition of cross sections into infrared regular and infrared singular parts, the latter defining the Sudakov cross section, is given in detail in section 2.2 . The structure of the Sudakov part, as outlined in this section, is derived in section 2.3 , whereby results of sections 1.4 - 1.6 and 2.2 are assembled.

1.4 Cross sections and parton densities, specific definitions and redundancies of the latter

The quantities $\sigma^{p\,(\bar{p})} \left[Q \, (\bar{Q}) \right]$ in eq. (29) are obtained from the parton densities of the incoming hadrons (proton and antiproton here), to be defined in a process independent way, upon a process specific convolution. We denote the process dependent quantities for virtual gauge boson production with the label D.Y. (for Drell - Yan processes) . They do not depend, to the relevant orders, on the particular virtual bosons (B) :

$$\sigma^{D.Y.\,H} (\underline{Q} ; x ; M) = \underline{Q}^{H} (x ; M) + \left\{ \begin{array}{l} \left[f_{qq}^{D.Y.} * \underline{Q}^{H} \right] (x ; M) + \\ \left[f_{qg}^{D.Y.} * g^{H} \right] (x ; M) \end{array} \right.$$

$$\sigma^{D.Y.\,H} (\underline{\bar{Q}} ; x ; M) = \underline{\bar{Q}}^{H} (x ; M) + \left\{ \begin{array}{l} \left[f_{qq}^{D.Y.} * \underline{\bar{Q}}^{H} \right] (x ; M) + \\ \left[f_{qg}^{D.Y.} * g^{H} \right] (x ; M) \end{array} \right.$$

$$f^{D.Y.}{}_{hh'} = f^{D.Y.}{}_{hh'} (x ; M) \quad ; \quad h , h' = q , g$$

$$H = p , \bar{p}$$

$$[f * F] (x) = \int_{x}^{1} d y / y \; f (x / y) F (y) \tag{30}$$

In eq. (30)

$$\sigma^{p.sp.\,H} (h) \quad , \quad h = \underline{Q} , \underline{\bar{Q}} , g$$

$$p.sp. = D.Y. , DI , \cdots$$

denotes a process specific, (Drell - Yan , deep inelastic , $\cdots$) , structure function of parton h inside the hadron H, evaluated at the scale M , whereas

$$h^H \quad , \quad h = \underline{Q} \, , \, \bar{\underline{Q}} \, , \, g$$

denotes the process independent density of parton h inside H, evaluated at the scale M .

The quantities $\sigma^{p.sp.\ H}(h)$ are measurable in principle and thus no freedom of choice, exists for them, contrary to the process independent parton densities h^H. The above two quantities are related, for any given process, through the convolution with the process specific functions $f^{p.sp.}{}_{hh'}$. We use the shorthand notation $p.sp. \rightarrow (\varrho)$:

$$\sigma^{(\varrho)\,H}(h\,;\,x\,;\,M) - h^H(x\,;\,M) = \left[f^{(\varrho)}{}_{hh'} * h'^H \right](x\,;\,M)$$
$$\sigma^{(\varrho)\,H}(h) = (\mathbf{1} + f^{(\varrho)}) * h^H \tag{31}$$

With the notation introduced in eq. (31) , the structure function $F_2^{e\,(\gamma)\,H}$, for deep inelastic scattering of electromagnetic currents, as function of the standard scaling variable $x = -q^2/(2\nu)$ and the (space like) momentum transfer $q = \sqrt{-q^2}$ is of the form :

$$F_2^{e\,(\gamma)\,H}(x\,;\,q) = x \sum\nolimits_\alpha e^2_{Q_\alpha} \left(\sigma^{2\,DI\,H}(Q_\alpha) + \sigma^{2\,DI\,H}(\bar{Q}_\alpha) \right) \tag{32}$$

For the quantities $\sigma^{2\,DI\,H}(h)$ in eq. (32) , eq. (31) defines the associated convolution functions $f^{2\,DI}{}_{hh'}$.

The redundancy in the definition of

$$f^{(\varrho)} \text{ and } h^H$$

is evident from eq. (31) . Let

$$h^H \, , \, f^{(\varrho)} \text{ and } \tilde{h}^H \, , \, \tilde{f}^{(\varrho)}$$

be two equivalent choices of parton densities and convolution functions.
Eq. (31) implies

$$\sigma^{(\varrho)H}(h) = (1 + f^{(\varrho)}) * h^H = (1 + \tilde{f}^{(\varrho)}) * \tilde{h}^H$$

$$\rightarrow \quad (1 + f^{(\varrho)})^{*-1} * (1 + \tilde{f}^{(\varrho)}) * \tilde{h}^H = (1 + \delta f) * \tilde{h}^H$$

δf : process independent, otherwise arbitrary

(33)

The convolution functions $f^{(\varrho)}$, $\tilde{f}^{(\varrho)}$, $\delta f(x;\mu)$ are expanded in powers of κ_μ :

$$f^{(\varrho)}(x;\mu) = \sum_{n=1}^{\infty} \kappa_\mu^n f_n^{(\varrho)}(x) \quad \text{and} \quad f^{(\varrho)} \rightarrow \tilde{f}^{(\varrho)} \rightarrow \delta f \tag{34}$$

To first order in κ_μ eq. (33) becomes :

$$\delta f_1 = \tilde{f}_1^{(\varrho)} - f_1^{(\varrho)} \tag{35}$$

Any set of parton densities h^H, $\tilde{h}^H$ satisfies the renormalization group equation, dropping the label H for brevity :

$$\left(\mu^2 \frac{\partial}{\partial \mu^2} + \beta(\kappa) \frac{\partial}{\partial \kappa} \right) h + P_{hh'} * h' = 0 \tag{36}$$

$$h = h(x; M, \mu, \kappa_\mu) \quad , \quad P_{hh'} = P_{hh'}(x; \kappa_\mu)$$

In eq. (36) P denotes the process independent Altarelli - Parisi evolution functions [2] . M denotes the reference scale, whereas μ stands for the dummy scale introduced through the definition of the strong coupling constant κ_μ . The evolution functions P are expanded in powers of κ_μ in the same way as the process specific convolution functions :

$$P(x;\kappa_\mu) = \sum_{n=1}^{\infty} \kappa_\mu^n P_n(x) \tag{37}$$

To match the relevant orders we consider here , terms up to second order in κ have to be retained in the expansion of P (eq. (37)) and β .
A specific choice of parton densities is realized by specific initial conditions for $M = \mu$.

We choose to define parton densities , denoted h^{ms} , by minimal subtraction of dimensionally infrared regluarized expressions. They satisfy the initial conditions :

$$\begin{aligned} &\partial_\kappa h^{ms}(x; M = \mu, \mu, \kappa_\mu) = 0 \quad \rightarrow \\ &h^{ms}(M, \mu, \kappa_\mu) = \Pi * \exp[E(M, \mu)] * h_0(\mu) \\ &h_0(x; \mu) = h^{ms}(x; M = \mu, \mu) \quad \text{independent of M} \\ &E(M, \mu) = \int_{\mu^2}^{M^2} d\mu'^2 / \mu'^2 \; P\{\bar{\kappa}(\mu')\} \end{aligned} \tag{38}$$

In eq. (38) the scaling variable x, the argument of the evolution functions E, P, and the densities h, is suppressed. The expression $\Pi * \exp *$ denotes the μ'^2 path ordered exponentiation of the convolution operation $*$.
$\bar{\kappa}(M)$ denotes the running coupling constant, satisfying the initial condition $\bar{\kappa}(M = \mu) = \kappa_\mu$.
A general alternative set of parton densities $\tilde{h}^H$ is evoluted with the same kernel $\Pi * \exp *$ as the minimal set (eq. (38)) , whereas the initial conditions are modified :

$$\begin{aligned} &\tilde{h}(\mu) = [1 + \delta f'(\kappa_\mu)] * h^{ms}(\mu) \\ &\tilde{h}(M, \mu, \kappa_\mu) = \Pi * \exp[E(M, \mu)] * \tilde{h}_0(M, \mu) \\ &\tilde{h}_0(x; M, \mu) = \tilde{h}(x; \mu, \mu, \bar{\kappa}(M)) \end{aligned} \tag{39}$$

The explicit dependence of the 'initial' parton densities $\tilde{h}_0(M, \mu)$ on M , through the running coupling constant $\bar{\kappa}(M)$ can only be eliminated reverting to the parton densities h^{ms} . The structure of the Sudakov cross section $d\sigma^S$ (eqs. (23 - 30)) demands in principle to evolute parton densities and the coupling constant not only to large M, but (nonperturbatively) to all M. The evolution scale (M) independent nature of the initial densities $h^{ms}(x; \mu)$ in eq. (38) thus considerably simplifies things.

For the parton densities $h = h^{ms}$, defined in eq. (38) , the functions $f^{2\,DI}$, f^{DY} relevant to the precision of the present discussion are :

$$f_{hh'}^{p.sp.}(x, M) = \bar{\kappa}(M) f_{1\,hh'}^{p.sp.}(x) \quad ; \quad p.sp. = DY, 2\,DI$$

$$f_{1qq}^{DY} = \frac{8}{3}\left[1 - x - \left(4 - \frac{\pi^2}{2}\right)\delta(1-x)\right]$$

$$f_{1qg}^{DY} = 1$$

$$f_{1qq}^{2\,DI} = \frac{8}{3}\left[\left(\frac{\log(1-x)}{1-x}\right)_+ (1+x^2) - \frac{3}{2}\left(\frac{1}{1-x}\right)_+ - \frac{1+x^2}{1-x}\log x + 3 + 2x - \left(\frac{9}{2} + \frac{\pi^2}{3}\right)\delta(1-x)\right]$$

$$f_{1qg}^{2\,DI} = [x^2 + (1-x)^2]\log\left(\frac{1-x}{x}\right) + 6x(1-x) \tag{40}$$

The convolution functions $f^{p.sp.}$ in eq. (40) , have been calculated first in ref. [3] , where an alternative definition of parton densities was adopted, which we denote by $\tilde{h} = h^{AEM}$.
To the relevant orders here, the specification of gluon densities beyond the leading order is not necessary. Thus we stick to the gluon densities in the h^{ms} scheme. The quantities $\tilde{f}^{(\varrho)} = f^{(\varrho)\,AEM}$ are related to the ms scheme in the following way :

$$f_1^{(\varrho)\,AEM} = f_1^{(\varrho)} + \delta f_1 \quad \rightarrow \quad \delta f_1 = -f_1^{2\,DI}$$
$$\text{to all orders : } h^{ms} = (\mathbf{1} + f^{2\,DI})^{*-1} * h^{AEM} \tag{41}$$

1.5 The Sudakov exponentiation

As stated in the introduction basic features of the Sudakov expnentiation were derived and discussed in references [6] - [9] .
In the context of the Sudakov exponentiation as performed in refs. ([8] , [9]) , it was pointed out by two of us [11], that the functional form of the Sudakov form factor in eq. (26) is the only consistent distribution which can be exponentiated

in impact parameter space. This comes about because the infrared regularization procedure allows for a redundancy in the definition of the distributions

$$
\begin{aligned}
&(f (q_T^2))_{+ s_T} \text{ ; for a test function } g (q_T^2) \quad : \\
&\left\langle (f)_{+ s_T} , g \right\rangle = \\
&\int_0^{s_T} d q_T^2 \, f (q_T^2) \, [g (q_T^2) - g (0)] + \int_{s_T}^{\infty} d q_T^2 \, f (q_T^2) \, g (q_T^2) \\
&f (q_T^2) \rightarrow \left(\frac{\log (q^2 / q_T^2)}{q_T^2} \right) \quad \text{and} \quad \rightarrow (1 / q_T^2)
\end{aligned}
\tag{42}
$$

Dimensional infrared regularization is to all orders exactly independent of the variable s_T in eq. (42) , which appears redundantly in the regulated singular distributions together with compensating regular terms. Thus any expression appearing in the Sudakov cross section satisfies the equation (to all orders) :

$$
\frac{\partial}{\partial s_T} d \sigma^S = 0 \longrightarrow \frac{\partial}{\partial s_T} S (b , q) = 0 \tag{43}
$$

Once the characteristic function delimiting the physical region ϑ_{phys} in eqs. (23) , (24) is factored out, the Sudakov form factor appears, to first order in κ , in the combined form :

$$S = S_{1\,s_T} + R_{1\,s_T}$$

$$S_{1\,s_T} = \frac{8}{3}\,\kappa_\mu \left[\int_0^{s_T} dq_T^2 / q_T^2 \{ 2 \log(q^2/q_T^2) - 3 \} \{ J_0(b q_T) - 1 \} + \right.$$

$$\left. + \int_{s_T}^{\infty} dq_T^2 / q_T^2 \{ 2 \log(q^2/q_T^2) - 3 \} J_0(b q_T) \right]$$

$$R_{1\,s_T} = -\frac{8}{3}\,\kappa_\mu \left[\log^2(s_T/q^2) + 3 \log(s_T/q^2) \right] \quad \rightarrow$$

$$\frac{\partial}{\partial s_T} \left[S_{1\,s_T} + R_{1\,s_T} \right] = 0 \tag{44}$$

Eqs. (43) and (44) imply that $d\sigma^S$ can only be a functional of the s_T independent combination $S = S_{1\,s_T} + R_{1\,s_T}$. The form of S in eq. (26) obtains upon choosing $s_T = q^2$. For this choice $R_{1\,s_T}$ vanishes.
The exponentiation adopted in refs. [8] and [9] :

$$1 + S_{1\,s_T} + R_{1\,s_T} \longrightarrow \exp S_{1\,s_T} \,(1 + R_{1\,s_T})$$
$$s_T = q_{T\,max}^2 \tag{45}$$

is analytically incorrect. Numerically this may not be conspicuous, for a limited range of center of mass energies $\sqrt{s}$.

We subdivide the q , q_T plane into the following regions, relative to the definitions in eq. (20) :

$$\begin{aligned}
&\text{throughout :} \quad q \gtrsim M_1 \approx 20\,GeV \;\; ; \;\; \Lambda_{\overline{MS}} \ll M_0 \approx 1\,GeV \\
&\text{sub-Sudakov region :} \quad 0 \leq q_T < M_0 \\
&\text{proper Sudakov region :} \quad M_0 \leq q_T \ll M_1 \\
&\text{perturbative region :} \quad M_1 \leq q_T
\end{aligned} \tag{46}$$

The subdivision into sub-Sudakov and proper Sudakov domains in eq. (46) takes into account the following :
resummation of the characteristic logarithmic factors

$$\frac{1}{q_T^2}\,\kappa^n(q_T)\,\log^m(q^2/q_T^2)\quad;\quad m\le 2n-1\quad;\quad n,m=1,2\cdots \tag{47}$$

for small q_T in the perturbative expansion of any given distribution $D(q_T)$ in q_T, e. g. :

$$D(q_T)\,|_{q,\,\bar\varphi_q,\,y_q,\,l_{1T}\ fixed} = \frac{d\sigma^S_{\alpha\beta}}{dq^2\,dq_T^2\,d\bar\varphi_q\,dy_q\,dl_{1T}} \tag{48}$$

to n-th order in $\kappa(q_T)$ relies on the appropriately exact knowledge of the expansion parameter κ. Contrary to the case of QED, originally discussed by Sudakov [13], the appearance of the running coupling constant, at arbitrarily small scales, invalidates this condition precisely in the sub-Sudakov region. The full nonperturbative structure of QCD is further necessary to evaluate parton densities at arbitrarily small scales.
Moreover, the incoherent reduction of the physical distribution to the subprocess level in terms of partons exactly collinear in momentum with the incoming hadrons, is invalidated in the sub-Sudakov region, where on the other hand the physical distributions are dominant.

In eq. (46), $M_0 \approx 1\ GeV$ denotes the minimum scale for which the collinear parton kinematics, and the running coupling constant are not significantly distorted by genuine nonperturbative QCD effects.

Any theoretically calculated physical distribution $D(q_T)$ is characterized by an a priori unknown theoretical error with respect to normalization and resolution relative to q_T in the sub-Sudakov region.
Even though the experimental resolution in q_T as well as the uncertainty in the experimental absolute efficiency for any given q_T may well be much smaller than

the theoretical respective uncertainties, it is only meaningful to compare theoretical and experimental distributions within the common resolution and normalization uncertainties. An eventual agreement of 'bare' theoretical and experimental values of $D\,(\,q_T = 0\,)$, e. g. , is fortuitous.

In the proper Sudakov region the logarithmic factors in eq. (47) can be resummed into an asymptotic expansion valid for $q_T \ll q\,,\ M_1$. The theoretical resolution with respect to q_T improves substantially in comparison with the sub-Sudakov region. Yet we know of no analytical estimate for this quantity.
The estimated theoretical resolution with respect to q_T is shown in figures 3a and 3b.
The different q_T domains detailed in eq. (46) do not provide a full covering. The proper Sudakov region falls short of joining in a theoretically satisfactory way to the perturbative region for $q_T \uparrow M_1 \approx 20GeV$. The onset of the perturbative region, denoted by M_1 in eq. (46), does in general depend on the quantities held fixed in the generic distribution $D\,(\,q_T\,)$ (eq. (48)) , i.e. :

$$q\,,\ \bar{\varphi}_q\,,\ y_q\,;\ s$$

For the above parameters in the ranges studied in this work we find

$$M_1 \approx 20GeV$$

except for extreme values, e. g. of the rapidity y_q , where the respective differential cross sections are extremely small.

We denote by transition region the domain

$$q_T < M_1 \quad ; \quad q_T \not\ll M_1 \tag{49}$$

In an attempt to estimate total cross sections (of Drell-Yan processes) from the perturbative regime [14] , it was pointed out, that the natural scale, which governs the running coupling constant as expansion parameter is q_T . In this work, all dependence of cross sections on the strong coupling constant, in the perturbative region is understood implying the substitution

$$\kappa \longrightarrow \kappa\,(\,q_T) \tag{50}$$

The Sudakov exponentiated expressions can be extended into the transition region (eq. (49)) . However the extrapolated expressions necessarily fail to approximate physical cross sections, by their incorrect analytic structure outside the proper

Sudakov region. Also we recall here, that the dominant scale governing the parton densities, is not necessarily given by the mass of virtual gauge bosons considered. In fact with increasing center of mass energy $\sqrt{s}$ the dominant contributions to the total production cross section will involve arbitrarily small scales. In addition the incoherent reduction of inclusive physical cross sections to subprocess cross sections will fail to remain an acceptable approximation. These properties are related to the theoretical uncertainties in the sub-Sudakov region detailed above. The deviations from perturbative QCD calculation, even when partially resummed, become large in particular in the limit $\sqrt{s} \rightarrow \infty$.

Positivity of the Sudakov exponentiated distributions is not guaranteed. This is illustrated in figure 1. We have sufficient control over the errors arising from our numerical calculations, to ascertain, that this feature is not an artefact.

All that can be done is to monitor the behaviour of the extrapolated Sudakov exponentiated distributions by the perturbative ones. This was done systematically, to first order in κ , in the unpublished thesis of one of us [15] . The quality of the osculation is displayed in figure 1.
The result is, that the two expressions - Sudakov and perturbative - are osculating to good precision in a definite range of q_T , near $M_1 \approx 20GeV$ for both values of $\sqrt{s}$ and throughout the q regions considered (eq. (21)) .

The matching of the two distributions is quite accurate, as illustrated in figure 1.

We note here, that the integrated q_T distributions, do not yield the total cross sections, as obtained by first integrating perturbative expressions over the final state variables on the subprocess level, with the scale governing parton densities held fixed, because of the effects inherent to the sub-Sudakov and transition regions. Again, numerically these two operations may approximately commute, yet the analytic expressions are necessarily different.

No new contributions are made to the discussion of the perturbative region, in principle. Nevertheless, the gauge bosons are kept perfectly virtual, the full (perturbative) multi differential cross sections, including all effects of Z , γ interference, are kept, whereupon phase space (sub) integrations are performed.

For the extended Sudakov region previous analyses ([8] , [9]) apply only (after appropriate modifications) to lepton spectra integrated over the transverse momenumtum l_{1T} :

$$\frac{d\sigma}{dq^2\, dq_T^2\, d\bar{\varphi}_q\, dy_q} = \int dl_{1T}\, \frac{d\sigma}{dq^2\, dq_T^2\, d\bar{\varphi}_q\, dy_q\, dl_{1T}} \tag{51}$$

The fully differential cross sections allow us to compute (to the relevant orders) the (projected) lepton transverse momentum distributions :

$$\frac{d\sigma^{p\bar{p}\to \ell_1 \ell_2}}{dE_T} \; ; \; \frac{d\sigma^{p\bar{p}\to \ell_1 \ell_2}}{dm_T} \tag{52}$$

$$E_T = l_{1T} \quad ; \quad m_T^2 = 2\, l_{1T}\, l_{2T}\, [\, 1 - \cos\varphi\, (\, \vec{l}_{1T}\, ,\, \vec{l}_{2T}\,)\,]$$

In principle we could study the effect of the limited experimental acceptance relative to the angle between the lepton momentum and the beam direction. The limitations in the numerical processing proved to be prohibitive at the present stage, since distributions integrated over all angles involve complete elliptic integrals, whereas a restricted angular range involves associated incomplete elliptic integrals. As discussed in section 3 and in ref. [16] , there exist powerful algorithms for the numerical evaluation of complete elliptic integrals, contrary to the situation for incomplete ones. The extension of our calculations to include angular lepton momentum acceptance cuts is beeing investigated.

The transverse lepton energy distributions show the characteristic Jacobian peak, including QCD corrections, and virtual gauge boson effects. These distributions retain their sensitivity to the gauge boson mass, while the restrictions present in the sub-Sudakov region do not manifest themselves , i. e. are considerably reduced, upon the projection, at the two center of mass energies considered. This feature confirms previous results stated in refs. [1] , [11] and [15] , where it was noted that the transverse lepton energy spectra essentially are insensitive to the choice of parton densities [19] , [20] , contrary to the corresponding behaviour of the q_T distributions in the sub-Sudakov region. The above features are demonstrated in figure 6 , figures 7a and 7b and figure 8 as compared to figures 3a and 3b .

1.6 Factorization of leptonic variables and electroweak couplings

We return to the leptonic factors (eqs. (23 - 30))

$$K_{\alpha\beta}\left[B, Q(\bar{Q}); \underline{q}, l_{1T}, y_{l_1}\right]$$

in eq. (28) to complete the discussion of the Sudakov cross section.
In the following all parton densities refer to the proton. The label ^{p} will be suppressed. Antiproton densities are related to proton densities by C or CP invariance.

The labels referring to specific channels

$$\alpha\beta, \left[B, Q(\bar{Q})\right] \tag{53}$$

determining

$$K_{\alpha\beta}\left[B, Q(\bar{Q}); \underline{q}, l_{1T}, y_{l_1}\right]$$

take the following values :

channel #	gauge bosons	subchannels α , β
$\mathrm{I}_{n\,m}$	W^-	d_m , $\bar{u}_n$
$\mathrm{I}'_{n\,m}$		$\bar{u}_n$, d_m
$\mathrm{II}_{n\,m}$	W^+	u_n , $\bar{d}_m$
$\mathrm{II}'_{n\,m}$		$\bar{d}_m$, u_n
III^{u}_{n}	Z , γ	u_n , $\bar{u}_n$
III'^{u}_{n}	Z , γ	$\bar{u}_n$, u_n
III^{d}_{n}	Z , γ	d_n , $\bar{d}_n$
III'^{d}_{n}	Z , γ	$\bar{d}_n$, d_n

(54)

$n, m = 1, 2, 3$

$u_n = (u, c, t)$; $d_n = (d, s, b)$

In eq. (53) the label Q refers to the channel numbers I, II, III, $\bar{Q}$ to I', II', III'.

The quantities

$$\eta_{\alpha\beta}\left[B, Q(\bar{Q})\right]$$

in eq. (28) can be reduced to the Drell - Yan specific densities of the proton only by C or CP invariance. In the following we will use the shorthand notation :

$$\sigma^{D.Y.\,p}\left[Q_\alpha(\bar{Q}_\alpha)\right] \rightarrow \sigma\left[Q_\alpha(\bar{Q}_\alpha)\right]$$

For the reaction channels in eq. (54) we obtain :

$$M_b = b_0 / b$$

$$\eta_{\alpha\beta}[B, Q] =$$

$$\begin{array}{lll|ll}
K^q(W^-) & \sum_{nm} |V_{nm}|^2\ \sigma(d_m; x_1^0; M_b)\,\sigma(u_n; x_2^0; M_b) & & \mathrm{I}_{nm} & W^- \\
K^q(W^+) & \sum_{nm} |V_{nm}|^2\ \sigma(u_n; x_1^0; M_b)\,\sigma(d_m; x_2^0; M_b) & & \mathrm{II}_{nm} & W^+ \\
K^u(Z,\gamma) & \sum_n \sigma(u_n; x_1^0; M_b)\,\sigma(u_n; x_2^0; M_b) & & \mathrm{III}_n^u & Z, \gamma \\
K^d(Z,\gamma) & \sum_n \sigma(d_n; x_1^0; M_b)\,\sigma(d_n; x_2^0; M_b) & & \mathrm{III}_n^d & Z, \gamma
\end{array} \qquad (55)$$

and similarly for $Q \rightarrow \bar{Q}$:

$$\eta_{\alpha\beta}[B, \bar{Q}] =$$

$$\begin{array}{lll|ll}
K^q(W^-) & \sum_{nm} |V_{nm}|^2\ \sigma(\bar{u}_n; x_1^0; M_b)\,\sigma(\bar{d}_m; x_2^0; M_b) & & \mathrm{I}'_{nm} & W^- \\
K^q(W^+) & \sum_{nm} |V_{nm}|^2\ \sigma(\bar{d}_m; x_1^0; M_b)\,\sigma(\bar{u}_n; x_2^0; M_b) & & \mathrm{II}'_{nm} & W^+ \\
K^u(Z,\gamma) & \sum_n \sigma(\bar{u}_n; x_1^0; M_b)\,\sigma(\bar{u}_n; x_2^0; M_b) & & \mathrm{III}'^u_n & Z, \gamma \\
K^d(Z,\gamma) & \sum_n \sigma(\bar{d}_n; x_1^0; M_b)\,\sigma(\bar{d}_n; x_2^0; M_b) & & \mathrm{III}'^d_n & Z, \gamma
\end{array} \qquad (56)$$

In eqs. (55) and (56) V_{nm} denote the elements of the Kobayashi-Maskawa-Cabibbo mixing matrix.

For the weak couplings we set

$$
\begin{aligned}
& g_W^2 = 4\sqrt{2}\, G_F\, m_W^2 \\
& m_Z = \frac{\bar{A}}{s_W\, c_W} = 91.16\ GeV \quad ; \quad \bar{A}^2 = \frac{A^2}{1 - \Delta r} \\
& A = \left(\frac{\pi\, \alpha}{\sqrt{2}\, G_F} \right)^{1/2} = 37.280\ GeV \\
& c_W = m_W / m_Z \quad ; \quad \bar{c}_W^2 = \frac{c_W^2}{1 + \Delta \varrho} \quad ; \quad \Delta \varrho \approx \frac{3\, m_t^2\, G_F}{8\, \pi^2 \sqrt{2}}
\end{aligned}
\tag{57}
$$

In eq. (57) we follow the conventions given in ref. [21] .

The leptonic factors K in eqs. (55) , (56) involve the kinematic decomposition

$$
\begin{aligned}
& K^x = K_1^x\, L_1 + K_2^x\, L_2 \\
& L_1 = \frac{1}{2} \left\{ (\lambda_1^+)^2 + (\lambda_2^-)^2 \right\} \quad ; \quad L_2 = \frac{1}{2} \left\{ (\lambda_1^-)^2 + (\lambda_2^+)^2 \right\} \\
& \lambda_r^{\pm} = \frac{\ell_r^{\pm}}{q^{\pm}} \quad ; \quad r = 1, 2
\end{aligned}
\tag{58}
$$

In eq. (58) $\ell_{1,2}$ denote the four momenta of lepton 1 , 2 respectively. We (arbitrarily) singled out lepton 1 in the respective reactions. Below we also list the quark or antiquark flavor inside the incoming proton, which takes part in the reaction subprocesses :

reaction	gauge boson	(anti)lepton 1 E	(anti)quark type $_p$ F
$I_{n\,m}$	W^-	e^-	d
$I'_{n\,m}$	W^-	e^-	$\bar{u}$
$II_{n\,m}$	W^+	e^+	u
$II'_{n\,m}$	W^+	e^+	$\bar{d}$
$III^{\,u}_{\,n}$	$Z\,,\,\gamma$	e^-	u
$III'^{\,u}_{\,n}$	$Z\,,\,\gamma$	e^-	$\bar{u}$
$III^{\,d}_{\,n}$	$Z\,,\,\gamma$	e^-	d
$III'^{\,d}_{\,n}$	$Z\,,\,\gamma$	e^-	$\bar{d}$

(59)

The factors $K^{\,x}_{1\,,\,2}$ in eq. (58) can be expressed by the left - and right handed electroweak couplings of the (anti)fermion pair E , F as specified for the different reactions in eq. (59) :

$$K^{\,x}_{1} = [\,K_{LL}\,(\,E\,,\,F\,) + K_{RR}\,(\,E\,,\,F\,)\,]$$

$$K^{\,x}_{2} = [\,K_{LR}\,(\,E\,,\,F\,) + K_{RL}\,(\,E\,,\,F\,)\,]$$

$$K_{XY}\,(\,E\,,\,F\,) = \left| \sum\nolimits_B \nu_B\, g^{\,E}_{X}\,(\,B\,)\, g^{\,F}_{Y}\,(\,B\,)\, \frac{1}{q^{\,2} - m^{\,2}_{B} + i\, m_B\, \Gamma^{\,B}_{tot}} \right|^2$$

$X\,,\,Y = L\,,\,R$

$B = W$ for reactions $I\,,\,I'\,,\,II\,,\,II'$; $B = Z\,,\gamma$ for reactions $III\,,\,III'$

$$\nu_W = g^{\,2}_{W} / 2 \;\;;\;\; \nu_Z = \frac{g^{\,2}_{W}}{\bar{c}^{\,2}_{W}} \;\;;\;\; \nu_\gamma = e^{\,2}$$

(60)

Since the combined couplings

$$G\,(\,B\,;E\,,\,F\,;\,XY\,)\;=\;g\,{}^{E}_{X}\,(\,B\,)\,g\,{}^{F}_{Y}\,(\,B\,) \tag{61}$$

enter only in the modulus of the expression in eq. (60) , an overall sign related to CP conjugation can be reversed.
The couplings associated to $K\,{}^{x}_{1\,,\,2}$ for the reactions in eq. (59) are listed below for virtual W production :

reaction	$B\,;\,E\,,F$	$K\,{}^{x}_{1}\,\rightarrow\,G$	$K\,{}^{x}_{2}\,\rightarrow\,G$
I	$W^{-}\,;\,e^{-}\,,\,d$	1	0
I'	$W^{-}\,;\,e^{-}\,,\,\bar{u}$	0	1
II	$W^{+}\,;\,e^{+}\,,\,u$	0	1
II'	$W^{+}\,;\,e^{+}\,,\,\bar{d}$	1	0

(62)

The extension to $\gamma\,,Z$ production is straightforward. [3]

The following CP relations hold :

$$\begin{aligned} &K\,{}^{x}_{r}\,:\,x\,\rightarrow\,I\,,\,II\,,\cdots,\,III'\;\;;\;\;r\,=\,1\,,\,2\\ &K\,{}^{J}_{1}\,=\,K\,{}^{J'}_{2}\;\;;\;\;K\,{}^{J'}_{1}\,=\,K\,{}^{J}_{2}\\ &J\,=\,I\,,\,II\,,\,III \end{aligned} \tag{63}$$

The leptonic kinematic factors $L_{\,1\,,\,2}$ in eq. (58) arise from the chiral couplings of virtual gauge bosons to leptons :

$$\begin{aligned} &q\,=\,\ell_{\,1}\,+\,\ell_{\,2}\quad\rightarrow\\ &\lambda\,{}^{\pm}_{r}\,=\,\frac{\ell\,{}^{\pm}_{r}}{q^{\,\pm}}\;\;;\;\;\vec{\lambda}_{\,r\,T}\,=\,\frac{\vec{\ell}_{\,r\,T}}{\mu_{\,T}\,(\,q\,)}\;\;;\;\;\lambda_{\,r\,T}\,=\,\left|\,\vec{\lambda}_{\,r\,T}\,\right|\;\;;\;\;r\,=\,1\,,\,2\\ &\cos\,(\,\Lambda_{\,q}\,)\,=\,q\,/\,\mu_{\,T}\,(\,q\,)\;\;;\;\;\sin\,(\,\Lambda_{\,q}\,)\,=\,q_{\,T}\,/\,\mu_{\,T}\,(\,q\,) \end{aligned} \tag{64}$$

[3] For a complete list of coupling constants we refer to the extended version of this paper [17] .

Momentum conservation implies :

$$\begin{aligned}
&\lambda_1^{\pm} + \lambda_2^{\pm} = 1 \quad ; \quad \vec{\lambda}_{1T} + \vec{\lambda}_{2T} = \vec{q}_T / \mu_T \\
&\cos^2(\Lambda_q) + 2\lambda_{1T} \sin(\Lambda_q) \cos\varphi_q = S_1 \quad ; \quad \lambda_{1T}^2 = P_1 \\
&\lambda_1^+ + \lambda_1^- = S_1 \quad ; \quad \lambda_1^+ \lambda_1^- = P_1 \\
&S_1 = 2\lambda_{1T} \cosh(\Delta y) \quad ; \quad \Delta y = y_{\ell_1} - y_q \\
&\lambda_1^{\pm} = \lambda_{1T} \exp(\pm \Delta y)
\end{aligned} \tag{65}$$

The final states variables q^μ , $E_T = \ell_{1T}$ specify the actual configuration only up to a twofold degeneracy, which is characterized by

$$\begin{aligned}
&(A) : y_{\ell_1} > y_q \\
&\lambda_1^+ |_A = \frac{1}{2}\left(S_1 + \sqrt{S_1^2 - 4P_1}\right) \quad ; \quad \lambda_1^- |_A = \frac{1}{2}\left(S_1 - \sqrt{S_1^2 - 4P_1}\right) \\
&(B) : y_{\ell_1} < y_q \\
&\lambda_1^+ |_B = \lambda_1^- |_A \quad ; \quad \lambda_1^- |_B = \lambda_1^+ |_A
\end{aligned} \tag{66}$$

The total Sudakov cross sections, differential with respect to the variables q^μ , E_T involves the sum over the discrete cases (A) and (B) in eq. (66) , whereas the lepton directional asymmetry involves the difference. The corresponding leptonic factors are :

$$\begin{aligned}
&\text{Sudakov cross section} : (K_1^x + K_2^x)(L_1 + L_2) \\
&\text{lepton asymmetry} : (K_1^x - K_2^x)(L_1 - L_2) \\
&L_1 + L_2 = S_1^2 - S_1 + 1 - 2P_1 \quad ; \quad \text{independent of } y_q \\
&L_1 - L_2 = sign(y_{\ell_1} - y_q)\sqrt{S_1^2 - 4P_1}
\end{aligned} \tag{67}$$

The leptonic factors for the Sudakov cross section (eqs. (58 - 67)) are the starting point to the following steps :

(i) they set the stage for the determination of the additional terms, which make up the full approximation to the differential cross section in the (extended) Sudakov region, to be completed in section 2.

(ii) they allow to extend the present calculations to include asymmetries from polarized incoming hadrons, and in principle from the observation of the polarization of final state leptons.

The rest of the paper is organized as follows :
Starting from eq. (23) we implement the Sudakov cross section to the complete expressions in section 2. These expressions are valid in the (extended) Sudakov region, and can readily be interpreted, upon appropriate simplifications, in the perturbative region (eq. (46)) .

$$\begin{aligned} d\sigma_{\alpha\beta} &= d\sigma^{S}_{\alpha\beta} + d\sigma^{R}_{\alpha\beta} \\ Z_{\alpha\beta} &= Z^{S}_{\alpha\beta} + Z^{R}_{\alpha\beta} \end{aligned} \tag{68}$$

The separate entries in eq. (68) are described in detail in section 2.

A selection of numerical results is presented in the final section 3 :

(i) total cross sections for the virtual gauge boson reactions, specified in the abstract, including an error analysis of the theoretical expressions

(ii) various projections of the differential cross sections, obtained from the partially integrated q_T^2 , $E_T = \ell_{1T}$ or q_T^2 , m_T distributions.

2 Construction of specific polarization projected differential cross sections [4]

As outlined in the discussion of dimensional infrared regularization in $4 + 2\varepsilon$ dimensions in (loew) approximation, (eqs. (9 - 17)) , we extend the QCD gauge couplings to include 2ε pseudoscalar gluon fields [12]

$$\tilde{g}^{t} \quad ; \quad t = 1, \cdots, 2\varepsilon$$

[4] For a complete discussion of all polarization dependence we refer to the extended version of this paper [17] .

with the (fourdimensionally reduced) couplings :

$$\mathcal{H}^{ps} = \tilde{g}_{s\epsilon} \sum_{t=1}^{2\epsilon} \bar{Q}_{\alpha}^{c'} i \gamma_5 \tilde{g}_A^t \left(\frac{\chi^A{}_{c'c}}{2} \right) Q_{\alpha}^{c} \tag{69}$$

We label the different reactions, starting with virtual W^- production, suppressing the flavor mixing indices :

I_{nm} , $I'_{nm} \longrightarrow r(I)$; $r \rightarrow (\alpha\beta)$:

r	α		β				r	α		β			
1	d	+	$\bar{u}$	$\rightarrow$	W^-	+ g	7	d	+	$\bar{u}$	$\rightarrow$	W^-	+ $\tilde{g}$
2	$\bar{u}$	+	d	$\rightarrow$	W^-	+ g	8	$\bar{u}$	+	d	$\rightarrow$	W^-	+ $\tilde{g}$
3	d	+	g	$\rightarrow$	W^-	+ u	9	d	+	$\tilde{g}$	$\rightarrow$	W^-	+ u
4	$\bar{u}$	+	g	$\rightarrow$	W^-	+ $\bar{d}$	10	$\bar{u}$	+	$\tilde{g}$	$\rightarrow$	W^-	+ $\bar{d}$
5	g	+	$\bar{u}$	$\rightarrow$	W^-	+ $\bar{d}$	11	$\tilde{g}$	+	$\bar{u}$	$\rightarrow$	W^-	+ $\bar{d}$
6	g	+	d	$\rightarrow$	W^-	+ u	12	$\tilde{g}$	+	d	$\rightarrow$	W^-	+ u

(70)

The reactions in eq. (70) are readily extended to virtual W^+ and Z ,γ production :

$$\begin{aligned} &I_{nm}\, I'_{nm} \longrightarrow II_{nm}\, II'_{nm} \longrightarrow III_n\, III'_n \\ &r(I) \longrightarrow r(II) \longrightarrow r(III^{u,d}) \end{aligned} \tag{71}$$

We do not give the associated reactions here. We refer to the extended version of this paper [17] for a complete discussion of all reactions and the associated cross sections.

The dimensionally regularized contributions of the processes in eq. (70) to the quantities $Z_{\alpha\beta}$ in eq. (68) are of the form :

$$Z_{\alpha\beta} \rightarrow Z_r \rightarrow Z_r^1 \; ; \quad r \rightarrow r(I)$$

$$Z_r^1 = C_r s_r \frac{1}{\Gamma_\gamma(1+\varepsilon)} \left(\frac{q_T^2}{\mu^2} \right)^\varepsilon \kappa_\mu Y_r^1 \frac{1}{q^2}$$

$$Y_r^1 = \int d\varrho(x_1, x_2) H_r(x_1, x_2) \frac{\left| \mathcal{M}_{(r)\ red} \right|^2}{8 x_1 x_2 s}$$

$$d\varrho(x_1, x_2) = dx_1 dx_2 \, \delta \left[(x_1 - \alpha^+)(x_2 - \alpha^-) - \frac{q_T^2}{s} \right] \tag{72}$$

In eq. (72) the label ^{1} denotes processes first order in κ_μ . The δ function includes the spectral condition

$$x_1 + x_2 \geq \alpha^+ + \alpha^-$$

and $\mathcal{M}_{(r)\ red}$ denotes the invariant matrix element of the subprocess r, whereby the strong coupling constant as well as the color flow is suppressed. The latter gives rise to the color factors C_r :

$$C_r = \begin{cases} \dfrac{8}{3} & \text{for} \quad r = 1, 2, 7, 8 \\ 1 & \text{otherwise} \end{cases} \tag{73}$$

In the case of emission or absorption of pseudoscalar gluons ($r = 7, \cdots, 12$), $\mathcal{M}_{(r)\ red}$ does not take into account the sum over pseudoscalar gluons

$$\tilde{g}^t \; ; \quad t = 1, \cdots, 2\varepsilon$$

This sum gives rise to the factor s_r in eq. (72) :

$$s_r = \begin{cases} 2\varepsilon & \text{for} \quad r = 7, \cdots, 12 \\ 1 & \text{otherwise} \end{cases} \tag{74}$$

$\Gamma_\gamma(z)$ in eq. (72) denotes the rationalized Gamma function :

$$\Gamma_\gamma(1+\varepsilon) = \exp(\gamma_E \varepsilon)\,\Gamma(1+\varepsilon) = \prod_{n=1}^{\infty}\left[\left(1+\frac{\varepsilon}{n}\right)e^{-\varepsilon/n}\right]^{-1}$$

$$\Gamma_\gamma(1+\varepsilon) = 1 + \frac{\pi^2\varepsilon^2}{12} + O(\varepsilon^3) \tag{75}$$

Upon the substitution $d \to d_m \;;\; u \to u_n$
in the reaction table in eq. (70), the KMC matrix elements V_{nm} can be transferred from the reduced matrix element $\mathcal{M}_{(r)\ red}$ to the combination of parton densities described by the quantities $H_r(x_1, x_2)$ in eq. (72) :

$$H_r(x_1, x_2) =$$

$$|V_{nm}|^2 \begin{cases} d_m(x_1, M)\ u_n(x_2, M) & \text{for } r = 1, 7 \\ \bar{u}_n(x_1, M)\ \bar{d}_m(x_2, M) & \text{for } r = 2, 8 \\ d_m(x_1, M)\ g(x_2, M) & \text{for } r = 3 \\ \bar{u}_n(x_1, M)\ g(x_2, M) & \text{for } r = 4 \\ g(x_1, M)\ u_n(x_2, M) & \text{for } r = 5 \\ g(x_1, M)\ \bar{d}_m(x_2, M) & \text{for } r = 6 \end{cases} \tag{76}$$

The scale M of the parton densities in eq. (76) is at present unspecified. The structure of H_r in eq. (76) goes over into the characteristic expressions in eqs. (55), (56) upon the appropriate substitutions of the reactions

$$r(I) \longrightarrow r(II) \longrightarrow r(III^{u,d})$$

For the full set of square moduli $\left|\mathcal{M}_{(r)\ red}\right|^2$ we refer to the extended version of this paper [17].

2.1 Inclusion of the reactions $r_{(0)}(I) = 1, 2$

We turn to the contributions of processes denoted by
$r_{(0)}(I) = 1, 2$, which involve only virtual gluons and no gluons at all, extending

the list of reactions in eq. (70) :

$$I_{nm}\ ,\ I'_{nm} \longrightarrow r_{(0)}\ (\ I\ )\quad ;\quad r_{(0)} \rightarrow (\ \alpha\beta\ )\ :$$

$r_{(0)}$	α	β		$r_{(0)}$	α	β
1	d	$\bar{u}$	$\rightarrow W^-$	2	$\bar{u}$	d	$\rightarrow W^-$

(77)

The reactions in eq. (77) yield additional contributions to the reduced cross sections denoted by $Z_{\alpha\beta}$ in eq. (72) :

$$Z_{\alpha\beta} \rightarrow Z_r \rightarrow Z_r^1 + Z_r^0\quad ;\quad r \rightarrow r_{(0)}\ (\ I\ )$$

$$Z_r^0 = \frac{1}{\Gamma_\gamma\ (\ 1 + \varepsilon\ )}\ \delta\ (\ q_T^2\ )\ Y_r^0\ \frac{1}{q^2}$$

$$Y_r^0 = (\ 1 - V_{DY}\ )\ H_r^0\ (\ x_1^0\ ,\ x_2^0\ )\ \frac{\left|\ \mathcal{M}^{\ 0}_{(r)\ \ red}\ \right|^2}{4\ x_1^0\ x_2^0\ s} \tag{78}$$

In eq. (78) V_{DY} denotes the vertex correction (to first order in κ_μ) , dimensionally (infrared) regularized for $q^2 > 0$, as appropriate for Drell - Yan processes :

$$V_{DY} = \left(\frac{8}{3}\ \kappa_\mu\right)\left(\frac{q^2}{\mu^2}\right)^{\varepsilon}\left[\frac{2}{\varepsilon^2} - \frac{3}{\varepsilon} + 8 - \pi^2\right] \tag{79}$$

$H_r^0\ (\ x_1^0\ ,\ x_2^0\ )$ denote appropriate products of unregularized parton densities :

$$H_r^0\ (\ x_1\ ,\ x_2\ ) =$$

$$|\ V_{nm}\ |^2 \begin{cases} d_m^{(0)}\ (\ x_1\ )\ \ u_n^{(0)}\ (\ x_2\ ) & \text{for}\quad r_{(0)} = 1 \\ \bar{u}_n^{(0)}\ (\ x_1\ )\ \ \bar{d}_m^{(0)}\ (\ x_2\ ) & \text{for}\quad r_{(0)} = 2 \end{cases} \tag{80}$$

Infrared regularization involves appropriate combinations of square moduli for reactions :

$$\begin{aligned} r_{(0)}(I) &= 1 \quad , \quad r(I) = 1, 3, 5, 7, 9, 11 \quad \text{and} \\ r_{(0)}(I) &= 2 \quad , \quad r(I) = 2, 4, 6, 8, 10, 12 \end{aligned} \tag{81}$$

For the full set of square moduli for the reactions $r_{(0)}(I, II, III^{u,d}) = 1, 2$ we refer to the extended version of this paper [17] .

2.2 Decomposition of cross sections into infrared finite and singular parts

The square moduli of the reduced amplitudes in eqs. (72) , (78) are further processed as follows :

$$\frac{\left| \mathcal{M}_{(r)\ red} \right|^2}{8 x_1 x_2 s} = \frac{q^2}{q_T^2} \Xi_{(r)}^{\ i} \quad , \quad \frac{\left| \mathcal{M}^{\ 0}_{(r)\ red} \right|^2}{4 x_1^0 x_2^0 s} = q^2 \Xi_0^{(r)\ i} \tag{82}$$

In eq. (82) the label ^{i} specifies polarizations of the quark and lepton pairs as well as gluons involved respectively in the reactions $r = 1 \div 6$.

Polarization dependent cross sections are decomposed according to the chain

$$\begin{gathered} Z_r = Z_r^1 + Z_r^0 \\ Z_r^0 \rightarrow Y_r^0 \rightarrow \Xi_{(r)}^{\ i} \quad , \quad Z_r^1 \rightarrow Y_r^1 \rightarrow \Xi_0^{(r)\ i} \end{gathered} \tag{83}$$

starting from the quantities Z_r^1 , Z_r^0 in eqs. (72) and (78) and substituting the square moduli $\Xi_0^{(r)\ i}$, $\Xi_{(r)}^{\ i}$ (eq. (82)) [17] .

The square moduli , $\Xi_0^{(r)\ i}$, $\Xi_{(r)}^{\ i}$ can be represented as sums of a factorizable and a nonfactorizable part with respect to the leptonic factors $K_{XY}(E, F)$ in eq. (60) :

$$\begin{gathered} \Xi_0^{(r)\ i} = \Xi_0^{G\ (r)\ i} \quad ; \quad \Xi_{(r)}^{\ i} = \Xi^{G\ (r)\ i} + \Xi^{\Delta\ (r)\ i} \\ d\sigma = d\sigma^G + d\sigma^\Delta \end{gathered} \tag{84}$$

In eq. (84) $\Xi^{\Delta\,(r)\,i}$ denote the nonfactorizable parts, which are infrared safe, i.e. integrable with respect to q_T for $\varepsilon \to 0$.
$\Xi^{G\,(r)\,i}$, $\Xi_0^{G\,(r)\,i}$ denote the factorizable parts, which contain all infrared singularities.

The factorizable quantities $\Xi^{G\,(r)\,i}$, $\Xi_0^{G\,(r)\,i}$ are of the form :

$$\Xi^{G\,(r)\,i} \,,\, \Xi_0^{G\,(r)\,i} = \sum_{\substack{XY\,k \\ k\,=\,1\,,\,2}} G_{k\,XY}^{(r)\,i}\, L_k\, K_{XY} \tag{85}$$

In eq. (85) L_k , $k = 1$, 2 denote the leptonic variables given in eq. (58), K_{XY} stand for the appropriate leptonic factors defined in eq. (60).

The factorizable and nonfactorizable parts in the decomposition
$d\sigma = d\sigma^G + d\sigma^\Delta$ are not uniquely determined by the structure of infrared singularities.

The coefficients $G_{k\,XY}^{(r)\,i}$ and the quantities $\Xi^{G\,(r)\,i}$, $\Xi_0^{G\,(r)\,i}$ in eq. (85) are given in the extended version of this paper [17] .

We specify the substitutions to be made in all terms forming $d\sigma^\Delta$ in eq. (84) :

$$\begin{aligned} \varepsilon &\to 0 \\ \kappa_\mu &\to \bar{\kappa}\,(q_T) \\ H_r\,(x_1\,,\,x_2\,;\,M) &\to H_r\,(x_1\,,\,x_2\,;\,q_T) \\ r &= 1 \div 6 \end{aligned} \tag{86}$$

With the substitutions in eq. (86) $d\sigma^\Delta$ can be constructed in the entire domain of tranverse momenta q_T . Of course for small momenta the expansion in $\bar{\kappa}\,(q_T)$ becomes untractable. This will develop into an interesting problem at very large values of $\sqrt{s}$. For $\sqrt{s} = 0.63$ and $1.8\ TeV$ the relative magnitude of $d\sigma^\Delta$ turns out to be small. The small scale contributions are well stabilized by freezing the strong coupling constant below a scale of $0.7 \div 1\ GeV$.

The contributions $d\sigma^\Delta$ are nevertheless essential in guaranteeing a smooth transition from the (extended) Sudakov domain to the perturbative region.

Redefining the quantities (eqs. (72) and (78)) :

$$z_r^{0,1} = Z_r^{0,1}\,\Gamma_\gamma\,(1+\varepsilon) \quad ; \quad z_r^{0,1} = \left(z_r^G\right)^{0,1} + \left(z_r^\Delta\right)^{0,1}$$

$$\bar{s}_r = \begin{cases} 1 \text{ for } r = 1 \div 6 \\ \varepsilon \text{ for } r = 7 \div 12 \end{cases} \tag{87}$$

the factorizable parts , $\left(z_r^G\right)^{0,1}$, in eq. (87) are of the form :

$$z_r^{G\,0} = \delta\,(q_T^2)\,(1 - V_{DY})\,y_r^{G\,0}$$

$$z_r^{G\,1} = \frac{1}{q_T^2}\left(\frac{q_T^2}{\mu^2}\right)^{\varepsilon} \kappa_\mu\, C_r\, \bar{s}_r\, y_r^{G\,1}$$

$$y_r^{G\,0} = H_r^0\,(x_1^0, x_2^0)\;\Xi_0^{G\,(r)}$$

$$y_r^{G\,1} = \int d\varrho\,(x_1, x_2)\, H_r\,(x_1, x_2)\;\Xi^{G\,(r)}$$

$$d\varrho\,(x_1, x_2) = \frac{dx_1}{x_1}\frac{dx_2}{x_2}\,\delta\left[(1 - R^+)(1 - R^-) - \frac{q_T^2}{q^2}\frac{x_1^0 x_2^0}{x_1 x_2}\right]$$

$$R^+ = \alpha^+ / x_1 \quad , \quad R^- = \alpha^- / x_2 \tag{88}$$

The square moduli $\Xi^{G\,(r)}$, $\Xi_0^{G\,(r)}$ in eq. (88) denote specific polarization sums of the quantities $\Xi^{G\,(r)\,i}$, $\Xi_0^{G\,(r)\,i}$ in eq. (85) . A complete list is given in ref. [17] .

With the terms labelled Δ out of the way, the remaining contributions in eq. (88) take the form :

$$y_r^{G\,0} = H_r^0 (x_1^0 , x_2^0) \qquad \begin{cases} K_+ \text{ for } r = 1 \\ K_- \text{ for } r = 2 \end{cases}$$

$$y_r^{G\,1} = J_r (x_1^0 , x_2^0 , q_T^2 / q^2) \qquad \begin{cases} K_+ \text{ for } r = \text{odd} \\ K_- \text{ for } r = \text{even} \end{cases} \tag{89}$$

In eq. (89) the separation of leptonic factors, including the resonance denominators, is evident.

The quantities J_r in eq. (89) involve the characteristic integrals, which are identical for all reactions I to III :

$$J_r (x_1^0 , x_2^0 , q_T^2 / q^2) =$$

$$\int d\varrho (x_1 , x_2) H_r (x_1 , x_2) \; G^{(r)} (R^+ , R^-) \tag{90}$$

All dependence of the factorizable cross section $d\sigma^G$ on the specific gauge boson and lepton channel

$$W^\pm , Z , \gamma \rightarrow e^\pm \overset{(-)}{\nu_e} a , e^+ e^-$$

is contained in the products of parton densities on one hand

$$H_r (x_1 , x_2) \quad , \quad H_r^0 (x_1^0 , x_2^0)$$

and in the leptonic factors K_+ , K_- (eq. (89)) on the other hand.

The functions $G^{(r)} (R^+ , R^-)$ in eq. (90) do not depend on the specific gauge boson and lepton channel, i.e. they are identical for reactions I , II , $III^{u,d}$. For a complete list we refer to ref. [17] .

The factorizable quantities $y_r^{G\,0}$, $y_r^{G\,1}$ in eq. (89) are further decomposed into infrared singular and regular parts :

$$y_r^{G\,0} = y_r^{S\,0} \quad , \quad y_r^{G\,1} = y_r^{S\,1} + y_r^{\delta\,1} \quad , \quad J_r = J_r^S + J_r^\delta$$
$$d\sigma^G = d\sigma^S + d\sigma^\delta \tag{91}$$

The decomposition in eq. (91) is the result of an asymptotic expansion of the integrals

$$J_r\left(x_1^0, x_2^0, q_T^2 / q^2\right)$$

for $q_T \to 0$, with q^2 , x_1^0 , x_2^0 held fixed :

$$J_r\left(x_1^0, x_2^0, q_T^2 / q^2\right) = J_r^S + J_r^\delta$$

$$J_r^S = \log\left[\frac{q^2}{q_T^2}\right] \mathcal{A}_r\left(x_1^0, x_2^0\right) + \mathbf{1}\, \mathcal{B}_r\left(x_1^0, x_2^0\right) \tag{92}$$

$$J_r^\delta\left(x_1^0, x_2^0, q_T^2 / q^2\right) = O\left(\log\left[\frac{q^2}{q_T^2}\right] q_T^2\right)$$

The specific form of J_r^δ is given in ref. [17] .
The decomposition $d\sigma^G = d\sigma^S + d\sigma^\delta$ as specified in eq. (91) is unique. J_r^S determines the Sudakov cross section.
The distributions corresponding to $d\sigma^\delta$ (eq. (91)) , as is the case for $d\sigma^\Delta$, are integrable with respect to q_T , and thus do not need infrared regularization. With the substitutions in eq. (86) $d\sigma^\delta$ can be constructed in the (extended) Sudakov region. For small transverse momenta the same comments apply as for $d\sigma^\Delta$. In the perturbative region , $d\sigma^\delta$, even though it can be computed without problems, has no physical meaning. This is a consequence of the infrared expansion, which fails to correctly reassemble $d\sigma^G$ from $d\sigma^S$ and $d\sigma^\delta$ for large values of q_T .

The coefficients $\mathcal{A}_r$, $\mathcal{B}_r$ in eq. (92) are of the form :

$$\mathcal{A}_r = G^{(r)}(1,1)\ H_r(x_1^0, x_2^0)$$

$$\mathcal{B}_r = j_*\ G^{(r)}(1,1)\ H_r(x_1^0, x_2^0) + I_r^0(x_1^0, x_2^0)$$

$$j_* = \log\left\{\frac{(1-x_1^0)(1-x_2^0)}{x_1^0 x_2^0}\right\} \tag{93}$$

$$G^{(r)}(1,1) = \begin{cases} 2 & \text{for } r = 1, 2 \\ 0 & \text{otherwise} \end{cases}$$

The specific form of the integrals $I_r^0(x_1^0, x_2^0)$ is given in ref. [17].

$\mathcal{B}_r$ involves the universal evolution of parton densities. The coefficients $\mathcal{A}_r$, $\mathcal{B}_r$ in eq. (93) are unique. They can be calculated for the simpler case of on shell gauge boson production, neglecting polarization effects. The full strength of the partial factorisation properties appears in the discussion of the polarized cross sections

$$d\sigma^S,\ d\sigma^\delta,\ d\sigma^\Delta$$

2.3 The Sudakov cross sections proper

We finally focus on $d\sigma^S$. With the terms labelled δ (and Δ) out of the way, we sum the contributions from

$$z_r^{S\,1},\ y_r^{S\,1},\ J_r^S$$

over even and odd values of r respectively, to match the two values $r_0 = 1, 2$. We drop the subscript 0 on the reaction channels in the following :

$$\hat{z}_r^0 = \delta(q_T^2)(1 - V_{DY})\,\hat{y}_r^0 \quad , \quad r = 1, 2$$

$$\hat{y}_r^0 = H_r^0(x_1^0, x_2^0) \quad , \quad r = 1, 2$$

$$\hat{z}_r^1 = \frac{1}{q_T^2}\left(\frac{q_T^2}{\mu^2}\right)^{\varepsilon} \kappa_\mu\, \hat{y}_r^1 \quad , \quad r = 1, 2 \tag{94}$$

$$\hat{y}_r^1 = \sum_{r'} C_{r'}\, \bar{s}_{r'}\, J_{r'}^S \begin{cases} r' \text{ odd} & \text{for } r = 1 \\ r' \text{ even} & \text{for } r = 2 \end{cases}$$

For the parton density products we use the notation, generic for all reactions :

$$H_r^0(x_1^0, x_2^0) = \begin{cases} q_1^0(x_1^0)\; q_2^0(x_2^0) & \text{for} \quad r = 1 \\ \bar{q}_2^0(x_1^0)\; \bar{q}_1(x_2^0) & \text{for} \quad r = 2 \end{cases} \tag{95}$$

KMC mixing angles and the specific flavor dependence are readily inserted in eq. (95) .
Furthermore we set :

$$D_P\, q(\bar{q})(x, M) = [P_{1\,qq} * q(\bar{q}) + P_{1\,qg} * g](x, M)$$

$$D_f\, q(\bar{q})(x, M) = \left[f_{1\,qq}^{DY} * q(\bar{q}) + f_{1\,qg}^{DY} * g\right](x, M) \tag{96}$$

In eq. (96) we translated the convolution functions inherent to $\mathcal{B}_r$ into the equivalent Altarelli - Parisi evolution functions $P_{hh'}$ and the Drell - Yan process specific convolution functions $f_{hh'}^{DY}$ discussed in
section 1 (eqs. (37) and (40)) .

With the notation introduced in eqs. (95) and (96) , the quantities $\hat{y}_r^0$, $\hat{y}_r^1$ in eq. (94) can be reduced to $r = 1$:

$$\hat{y}^{\,0} = \hat{y}^{\,0}_{1} \quad , \quad \hat{y}^{\,1} = \hat{y}^{\,1}_{1} \quad , \quad x^{\,0}_{j} = z_{j} \quad , \quad j = 1 \, , \, 2$$

$$\hat{y}^{\,0} = q^{\,0}_{1} (z_{1}) \, q^{\,0}_{2} (z_{2})$$

$$\hat{y}^{\,1} = A + B \quad , \quad A = a \, q_{1} (z_{1} \, , \, M) \, q_{2} (z_{2} \, , \, M)$$

$$a = \frac{8}{3} \left[2 \log \left\{ \frac{q^{\,2}}{q^{\,2}_{T}} \right\} - 3 + \varepsilon \, (8 - \pi^{\,2}) \right] \tag{97}$$

$$B = \left[\begin{array}{l} q_{1} (z_{1} \, , \, M) \quad [D_{P} + \varepsilon \, D_{f}] \, q_{2} \, (z_{2} \, , \, M) + \\ \\ [D_{P} + \varepsilon \, D_{f}] \, q_{1} \, (z_{1} \, , \, M) \quad q_{2} (z_{1} \, , \, M) \end{array} \right]$$

$$r = 1 \rightarrow r = 2 \quad \leftrightarrow \quad q_{1} \, , \, q_{2} \rightarrow \bar{q}_{2} \, , \, \bar{q}_{1}$$

The factor a in eq. (97) matches in its structure the vertex correction.

We next combine eqs. (94) and (97) :

$$\hat{z}^{\,0} = \hat{z}^{\,0}_{1} \quad , \quad \hat{z}^{\,1} = \hat{z}^{\,1}_{1}$$

$$\hat{z}^{\,0} = \delta (q^{\,2}_{T}) (1 - V_{DY}) \, q^{\,0}_{1} (z_{1}) \, q^{\,0}_{2} (z_{2})$$

$$\hat{z}^{\,1} = \kappa_{\mu} \, \frac{1}{q^{\,2}_{T}} \left(\frac{q^{\,2}_{T}}{\mu^{\,2}} \right)^{\varepsilon} [a (q^{\,2} / q^{\,2}_{T}) \, q_{1} (z_{1} \, , \, M) \, q_{2} (z_{2} \, , \, M) + B] \tag{98}$$

Once the leptonic factors and nonleading contributions $d \sigma^{\,\delta}$ and $d \sigma^{\,\Delta}$ are out of the way, the structure of infrared and collinear singularities determines the expressions in eq. (98) exactly. They indeed coincide with the corresponding expressions in refs. [8] and [9] . The Sudakov exponentiation and the reconstruction of the differential cross section differs in the following from previous analyses.

For finite center of mass energy, the range of q_{T} values is limited by $q_{T \, max}$.

The universal structure of the expressions in eq. (98) is maintained provided the characteristic function $\vartheta (q_{T\,max} - q_T)$
is factored out, together with the leptonic factors.
Next we consider the Fouriertransformation $\mathcal{F} : F \longrightarrow \tilde{F}$ of functions (distributions) to impact parameter space :

$$\mathcal{F} : F \longrightarrow \tilde{F}$$

$$\tilde{F} = \frac{1}{\pi} \int d^2 q_T \exp (i \vec{b} \vec{q}_T) F \quad , \quad F = \frac{1}{4\pi} \int d^2 b \exp (- i \vec{b} \vec{q}_T) \tilde{F}$$

for axially invariant distributions :

$$\hat{F} = \int d q_T^2 J_0 (b q_T) F \quad , \quad F = \frac{1}{4} \int d b^2 J_0 (b q_T) \tilde{F}$$

(99)

In impact parameter space eq. (98) becomes :

$$\hat{z}^0 \rightarrow \tilde{z}^0 \quad , \quad \hat{z}^1 \rightarrow \tilde{z}^1 \quad ; \quad \tilde{z}^0 = (1 - V_{DY}) H_{12}^0$$

$$\tilde{z}^1 = \frac{8}{3} \kappa_\mu \left[2 \tilde{F}_3 + (-3 + \varepsilon (8 - \pi^2)) \tilde{F}_2 \right] H_{12} + \kappa_\mu B \tilde{F}_2$$

$$H_{12}^0 = q_1^0 (z_1) q_2^0 (z_2) \quad , \quad H_{12} = q_1 (z_1 , M) q_2 (z_2 , M)$$

$$\tilde{F}_2 = \left(\frac{q^2}{\mu^2} \right)^\varepsilon \frac{1}{\varepsilon} \beta^{-\varepsilon}$$

$$\tilde{F}_3 = \left(\frac{q^2}{\mu^2} \right)^\varepsilon \left[\frac{1}{\varepsilon^2} + \frac{1}{\varepsilon} \log \beta \right] \beta^{-\varepsilon}$$

$$\beta = \frac{b^2 q^2}{b_0^2} \quad , \quad b_0 = 2 e^{-\gamma_E}$$

(100)

By means of the distributions

$$\tilde{\Psi}_2 = \tilde{F}_2 - \left(\frac{q^2}{\mu^2} \right)^{\varepsilon} \frac{1}{\varepsilon} \rightarrow - \log \beta$$

$$\tilde{\Psi}_3 = \tilde{F}_3 - \left(\frac{q^2}{\mu^2} \right)^{\varepsilon} \frac{1}{\varepsilon^2} \rightarrow - (\log \beta)^2 / 2 \tag{101}$$

which have a well fefined limit for $\varepsilon = 0$, and modulo higher orders in κ_μ , eq. (100) can be cast to the form :

$$\tilde{z}^0 = H^0_{12} - V_{DY} \; H_{12}$$

$$\tilde{z}^1 = \left\{ \begin{array}{l} \left[V_{DY} + \dfrac{8}{3} \kappa_\mu \left(2 \tilde{\Psi}_3 - 3 \tilde{\Psi}_2 \right) \right] H_{12} + \\ \\ + \kappa_\mu \left[\dfrac{1}{\varepsilon} + \log \left\{ \dfrac{b_0^2}{(b\mu)^2} \right\} \right] B \end{array} \right\} \tag{102}$$

It follows from eq. (102) that, modulo higher orders in κ_μ , the terms proportional to V_{DY} cancel in the sum $\tilde{z} = \tilde{z}^0 + \tilde{z}^1$.

This is due to cancellation of infrared divergencies on one hand and the appropriate choice of identity parts of the evolution functions P_{qq} , f_{qq} on the other hand.

Then eq. (102) becomes :

$$\tilde{z} = \left[1 + \frac{8}{3} \kappa_\mu \left(2 \tilde{\Psi}_3 - 3 \tilde{\Psi}_2 \right) \right] \sigma (q_1 ; z_1) \sigma (q_2 ; z_2)$$

$$\sigma (q ; z) = q^0 (z) + \kappa_\mu \left\{ \left[\frac{1}{\varepsilon} + \log \left\{ \frac{b_0^2}{(b \mu)^2} \right\} \right] D_P + D_f \right\} q (z , M) \tag{103}$$

Eq. (103) is as far as one can go to first order in κ_μ . $\tilde{z}$ is to be rendered renormalization group invariant and the scale M in the respective parton densities in eq. (103) remains to be determined.

This is achieved by the following substitutions in eq. (103) :

$$M \to \mu \quad , \quad M_b = \frac{b_0}{b}$$

$$q^0 (z) = q (z , \mu) - \kappa_\mu \frac{1}{\varepsilon} D_P \, q (z , \mu) \tag{104}$$

$$\to \quad \sigma (q ; z) = [1 + \bar{\kappa} (M_b) D_f] \; q (z , M_b)$$

$$q = q^{ms} \quad , \quad \sigma = \sigma^{DY}$$

In the expression for σ^{DY} in eq. (104) the specific parton densities correspond to minimal (dimensional infrared) subtraction, as discussed in section 1.4 . We recall that the process dependent distributions σ^{DY} are independent of the specific definition of parton densities.

The Sudakov form factor, appearing in the expression for $\tilde{z}$ in eq. (103) , remains to be rendered renormalization group invariant. Upon the substitution $M \to M_b$ we obtain :

$$\tilde{z} = [\, 1 + S\,(\, b\,,\, q^{\,2}\,)\,]\; H^{\,b}_{12}$$

$$S\,(\, b\,,\, q^{\,2}\,) = \frac{8}{3}\,\kappa_{\,\mu}\;\left[\, 2\,\tilde{\Psi}_{\,3} - 3\,\tilde{\Psi}_{\,2}\,\right] = -\,\frac{8}{3}\,\kappa_{\,\mu}\;[\,(\,\log\,\beta\,)^{\,2} - 3\,\log\,\beta\,]$$

$$H^{\,b}_{12} = \sigma^{\,DY}\,(\, q_{\,1}\,;\, z_{\,1}\,,\, M_{\,b}\,)\;\sigma^{\,DY}\,(\, q_{\,2}\,;\, z_{\,2}\,,\, M_{\,b}\,) + O\,(\,\kappa^{\,2}_{\,\mu}\,) \tag{105}$$

The Fouriertransform of (only) $S\,(\, b\,,\, q^{\,2}\,)$ back to $q_{\,T}$ space yields :

$$\tilde{S}\,(\, q_{\,T}\,,\, q^{\,2}\,) = \frac{8}{3}\;\hat{S}\quad,\quad \hat{S} = \kappa_{\,\mu}\;(\, 2\,\Psi_{\,3} - 3\,\Psi_{\,2}\,)$$

$$\hat{S} = \kappa_{\,\mu}\left(\left[\, 2\,\log\left\{\frac{q^{\,2}}{q^{\,2}_{\,T}}\right\} - 3\right]\;\frac{1}{q^{\,2}_{\,T}}\right)_{+\,q^{\,2}} \tag{106}$$

The scale dependence and specific form of the term $H^{\,b}_{12}$ in eq. (105) is determined exactly by the definite choice of the infrared finite cross sections $d\,\sigma^{\,\delta}$ and $d\,\sigma^{\,\Delta}$ as discussed in section 2.2 . Infrared singularities determine the distribution $\hat{S}$ in eq. (106) uniquely, in particular the subtraction point $q^{\,2}$.

The structure of the leading multiple gluon emission amplitudes in the Sudakov approximation implies the following completion of eq. (106) [11] , [22] :

$$\kappa_{\,\mu} \rightarrow \bar{\kappa}\,(\, q_{\,T}\,)$$

$$\tilde{S} \rightarrow \frac{8}{3}\;\bar{\kappa}\,(\, q_{\,T}\,)\left(\left[\, 2\,\log\left\{\frac{q^{\,2}}{q^{\,2}_{\,T}}\right\} - 3\right]\;\frac{1}{q^{\,2}_{\,T}}\right)_{+\,q^{\,2}} \tag{107}$$

The expression for $\tilde{S}$ in eq. (107) is the final form which can be obtained from a renormalization group improved first order calculation. Although arbitrarily high orders are resummed, a second order calculation indeed modifies the subleading logarithmic terms [27] .

Let S denote the Fouriertransform of $\tilde{S}$ in eq. (107) . The replacement

$$(1 + S) \rightarrow \exp S \tag{108}$$

yields the structure of the Sudakov form factor, and of the distribution $\tilde{z}$ (eqs. (105) , (107)) discussed in section 1.5 (eq. (44)) :

$$\tilde{z} \rightarrow \exp \left[S (b , q^2) \right] H^{b}_{12}$$

$$S (b , q^2) = \frac{8}{3} \int d q_T^2 / q_T^2 \ \bar{\kappa} (q_T) \left[2 \log \left\{ \frac{q^2}{q_T^2} \right\} - 3 \right] \times$$

$$\times \begin{cases} \left[J_0 (b q_T) - 1 \right] & \text{for} \quad q_T^2 \leq q^2 \\ J_0 (b q_T) & \text{for} \quad q_T^2 > q^2 \end{cases}$$

$$H^{b}_{12} = \sigma^{DY} (q_1 ; z_1 , M_b) \ \sigma^{DY} (q_2 ; z_2 , M_b) + O (\kappa_\mu^2) \tag{109}$$

3 Numerical Results

One objective of this work is to obtain a reference set of projected cross-sections for the three inclusive reactions discussed in this paper, our interest being mainly focused on distributions directly useful for the W and Z mass determination at the Fermilab Tevatron. The results presented in this chapter are derived without taking any experimental constraint (detector resolution, cuts, ...) into account[5]. This prevents their direct utilization for a precise determination of the weak vector boson masses; however they do provide a clean way to test the theoretical approximations on which the Monte-Carlo programs used for the data analysis are based. For this purpose, the numerical treatment involved in our evaluation of the projected cross-sections is here extensively described.

A summary of our input parameters choice is given in table 1; let us first discuss it. Our treatment of the QCD running coupling constant α_s is taken from the paper by G.Altarelli et al. [8]; it is a leading order parametrization with charm and beauty thresholds and with freezing in the low momentum region (controlled by some parameter a). We took $a = 10$, $m_c = 1.35\,\text{GeV}$ and $m_b = 5.3\,\text{GeV}$. This

[5]It turns out that the implementation of these constraints would result in a prohibitive increase of the CPU time required by the numerical integration of the differential cross-section.

α_s parametrization is unambiguously fixed by the requirement that it matches at a scale of 5 GeV the α_s parametrization of the chosen set of parton densities.
All results in this paper are derived with parton densities from M.Diemoz et al. [18]. We used three density sets corresponding to three different values of $\Lambda_{4flavors,\overline{MS}}$, namely 160 MeV, 260 MeV and 360 MeV (these sets will be referred to as DFLM g160,...), in order to test the sensitivity of the result with respect to Λ^{QCD} and to the choice of densities. The latter are mainly extracted from neutrino deep inelastic scattering data at a reference scale $\mu = \sqrt{10}\,\text{GeV}$; all next-to-leading corrections in α_s are included both in extracting them and in calculating their evolution; a *numerical* form of these densities is provided for $x \in (5 \cdot 10^{-5}, 1)$ and $Q^2 \in (10, 5 \cdot 10^9)\,\text{GeV}^2$. For these parametrizations, regularized quark densities are defined by demanding that the structure function F_2 of deep inelastic scattering maintains the same form as in the naive parton model. This regularization scheme differs from the minimal subtraction scheme we used [eq.(38)]; however, equation (41) gives the explicit relation between the densities obtained from both definitions, so that we were able to take this difference into account when deriving our numerical results. This difference is illustrated for the up quark density in figure 2.
The complete expression for the fully differential cross-section $d\sigma$, for any of the three inclusive reactions described in the abstract, is [$d\sigma^{irp} \doteq d\sigma^G(\epsilon = 0)$]:

$$d\sigma \doteq \theta(q_T^{lim} - q_T) \cdot (d\sigma^S + d\sigma^\delta + d\sigma^\Delta) + \theta(q_T - q_T^{lim}) \cdot (d\sigma^{irp} + d\sigma^\Delta) \qquad (110)$$

The quantities $d\sigma^{irp}$,$d\sigma^\delta$ and $d\sigma^\Delta$ (pure perturbative parts of $d\sigma$) contain the strong coupling and the parton densities evaluated at a scale which is not determined on the level of our calculations. As discussed in sections 1.5 and 2.2 we *chose* to identify this scale with q_T in order to obtain a smooth transition between the resummed $(d\sigma^S + d\sigma^\delta + d\sigma^\Delta)$ and the pure perturbative $(d\sigma^{irp} + d\sigma^\Delta)$ forms of the cross-section. As a consequence, the explicit value of q_T^{lim} is of little importance, as long as it lies in the intermediate q_T-region where both these forms are valid and nearly coincide (for example, at $\sqrt{s} = 630\,\text{GeV}$, a value of q_T^{lim} running from 16 to 25 GeV induces a relative variation of σ_{tot}^W which is not larger than a few per mille — σ_{tot}^W is the total inclusive cross-section for $e\nu$ pairs production through W).
The three quantities $\alpha\,(1/137.036)$, $G_F\,(1.16639 \cdot 10^{-5}\ \text{GeV}^{-2})$ and m_Z being well measured, we chose them, as well as the top mass (m_t) and the Higgs mass (m_H), as a set of independant electroweak parameters. From this set, for a specific choice of m_t and m_H and for three fermion generations, we obtain the values shown in table 1:

- The Weinberg angle $\sin^2\theta_W \doteq \overline{s}_W^2$, according to the definition of W.Hollik [21] [see also eq.(57)]; the leading order electroweak corrections are included. We point out that the neutral current couplings we used are expressed in terms of $\overline{s}_W^2$.

- The total Z width Γ_Z, including leading order electroweak and QCD corrections (with $\alpha_s(M_Z^2) = 0.12$). From Ref. [23].

- The W mass m_W, including leading order electroweak corrections. From Ref. [24].
- The total W width Γ_W, including leading order QCD corrections. Calculated by one of us (C.Greub [12]).

In fact our numerical results are practically not sensitive to the value of m_H. Moreover, sensitivity to the choice of m_t is weak, but for the results which explicitly depend on the W mass; for instance, the relative variation of σ_{tot}^W for m_t going from 90 GeV to 200 GeV is about 2%.

Obtaining integrated distributions — such as $\frac{d\sigma}{dl_{1T}}$ — from the *fully* differential cross-section $d\sigma$, defined by equation (110), turned out to be a non trivial numerical problem. For this purpose we developed a set of FORTRAN routines for use on the CRAY-2 machine of the EPFL in Lausanne; the task of these routines was divided into two steps:

1. The distributions $\frac{d^3\sigma}{dq^2\, dq_T^2\, df}$ ($\doteq d^3\sigma_f$), for $f \in (l_{1T}, l_{2T}, m_T)$, are worked out in some (q, q_T, f)-region $\mathcal{D}_f$ and for some specific choice of the input parameters (produced weak vector boson, parton densities parametrization — in a analytic or numerical form, $\sqrt{s}$, ...). The values of weak vector boson mass and width, as well as electroweak couplings, enter as free parameters in the expression of $d^3\sigma_f$ so obtained. For the results presented in this paper:

$$\sqrt{s} \in \{0.63, 1.8\}\,\text{TeV}$$

$$q \in \begin{cases} (20, 140)\,\text{GeV} & \text{for } \sqrt{s} = 0.63\,\text{TeV} \\ (50, 140)\,\text{GeV} & \text{for } \sqrt{s} = 1.8\,\text{TeV} \end{cases}$$

$$l_{1T}, l_{2T}, q_T \in (0, 100)\,\text{GeV} \quad ; \quad m_T \in (0, 140)\,\text{GeV}$$

2. Numerical integration of $d^3\sigma_f$ over some subset $\mathcal{D}'$ of $\mathcal{D}_f$.

Mean CRAY-2 CPU time used to obtain $d^3\sigma_f$, for one set of parameters, was about 90 minutes (this time is understood with full vectorization, which increases the speed by a factor of 9 with respect to scalar mode); the time used by the second step is negligible. The relative error on the *total* cross-section introduced by the above *numerical* procedure was estimated to be at most 1% (this value does not include the effect of phase space truncation induced by the constraint $q \in \mathcal{D}_f$); an error of the same magnitude is expected on $d^3\sigma_f$ evaluated at any point of the region where the bulk of the cross-section lies.
Let us now briefly describe the way $d^3\sigma_f$ is obtained (to fix the notation $f = l_{1T}$ and a reaction with W production is considered). The fully differential cross-section $d\sigma$ [eq.(110)] contains the kinematic factor $\delta(q^2 - 2ql_1)$; from that we integrate out y_l and obtain the factorized form (111) in which φ_q and y_q integrations are disentangled.

This is an important numerical simplification which is no more valid if the additional phase space constraints derived from experimental cuts are taken into account.

$$\frac{d^3\sigma^W}{dq^2\, dq_T^2\, dl_{1T}} \sim \sum_i \mathcal{F}_i(M_W, \Gamma_W, G_F; q^2) \cdot \mathrm{Lept}_i(q_T, q^2, l_{1T}) \cdot \mathrm{Hadr}_i(q_T, q^2) \qquad (111)$$

The weak vector boson propagator and the electroweak couplings enter in $\mathcal{F}_i$. The quantities Lept_i are φ_q-integrals which can be analytically worked out. Hadr_i are parton densities and strong coupling dependant quantities which can be expressed in terms of double integrals over (y_q, z_1) and of the backward Fourier transformation:

$$\frac{1}{2}\int_0^\infty b\, db\, \exp[S(b,q)]\, J_0(bq_T)\, \Sigma(b,q,q_T) \qquad (112)$$

$$\Sigma \doteq \int_{P.S.} dy_q \cdot \sum_{\alpha\beta} [\tilde{H}_{\alpha\beta}(Q, x_1^0, x_2^0, \frac{b_0}{b}) + \tilde{H}_{\alpha\beta}(\bar{Q}, \ldots)]$$

(J_0 is the Bessel function of order 0, S(b,q) is the Sudakov form factor [eq.(26)], P.S. means phase space and $\tilde{H}_{\alpha\beta}$ is defined by eq.(29)). (y_q, z_1)-integrations are worked out over the whole allowed phase space region with the help of the adaptative NAG routine D01ATF; b-integration, restricted to the interval $(10^{-4}, 20)\,\mathrm{GeV}^{-1}$, as well as the Sudakov form factor S(b,q), are evaluated with the adaptative NAG routine D01AUF (especially suited for oscillating integrands). Because parton densities evaluated at a scale b_0/b enter in the expression of $\tilde{H}_{\alpha\beta}$, and the form of these densities is only known above some scale Q_0, $\Sigma(b,q,q_T)$ has to be extrapolated with respect to b from the value $b_{crit} = b_0/Q_0$ up to $b_{max} = 20\,\mathrm{GeV}^{-1}$ (for DFLM parametrization $b_{crit} \approx 0.35\,\mathrm{GeV}^{-1}$). As a first step we built a smooth extrapolating function $\bar{\Sigma}(b,q,q_T)$ which is linear in $\log(b)$. However, when the sea partons dominate the Σ evolution, this extrapolating function may become smaller than $\bar{\Sigma}_{vv}$, $\bar{\Sigma}_{vv}$ being the valence parton contribution to $\bar{\Sigma}$. In such a case our final function $\bar{\Sigma}$ is a smooth interpolation between $\Sigma(b \le b_{crit}, q, q_T)$ and $\bar{\Sigma}_{vv}(b \ge \bar{b}, q, q_T)$, for some $\bar{b} \ge b_{crit}$. We checked that the details of the above procedure are of little numerical importance for any results, but for the q_T *non* integrated distributions evaluated at small q_T and at small q — typically, for q around 50 GeV, the sensitive q_T region is below 2 GeV and then slowly grows when q becomes smaller. In any case, in this latter region, our calculations become less reliable because of the lack of theoretical informations about phenomena such as the intrinsic transverse momentum of partons inside the nucleon, the low scale behaviour of the strong coupling or higher twist effects. Note finally that some brutal solution, such as setting b_{max} equal to $\frac{b_0}{Q_0}$ or, to a lesser measure, freezing the partons scale below Q_0, results in some artificial oscillation of the q_T-distribution.

From the previously described formalism and input we obtain the normalized distributions for the transverse momentum of the W (*i.e.* W^+ or W^-) and of the (Z,γ)

bosons

$$\frac{dR}{dq_T^2} = \left(\int_0^{100} dq_T^2 \frac{d\sigma}{dq_T^2}\right)^{-1} \cdot \left(\frac{d\sigma}{dq_T^2}\right)$$

which are plotted in figures 3a and 3b. The dependence on parton densities and Λ was studied by using the three parton density sets DFLM g160,g260 and g360; it is specially strong in the small q_T region, as indicated by the error bars in figure 3a, but then decreases to reach the level of a few per cent in the hard q_T region ($q_T > 30\,\text{GeV}$). In this latter region, the $O(\alpha_s^2)$ calculations of Arnold and Reno [5], with their stated uncertainties, are displayed[6]. Together with the above discussed dependence they give a good idea of the theoretical uncertainty of our q_T-distribution.

In table 2 our values of the total cross-section for the inclusive lepton pair production ($e\nu, ee$) through virtual W ($\sigma_{tot}^{W^+}$, $\sigma_{tot}^{W^-}$) and Z (σ_{tot}^{Z}), produced in $p\bar{p}$ collisions, are compared with the experimental results obtained by the UA2 collaboration at 0.63 TeV [25] and the preliminary results from the CDF collaboration at 1.8 TeV [26]. Our theoretical values are obtained by integration over the phase space region defined by $\sqrt{q^2} \in (50, 140)\,\text{GeV}$. Moreover, the photon coupling is set to zero when deriving σ_{tot}^{Z}: even though the *measured* cross-section for charged lepton pair production includes the γ exchange and the $Z\gamma$ interference contribution, the published experimental results have been corrected, so that they do not contain these terms any longer. Their importance can be read off from figure 4 where the relative contribution of these terms to the quantity $\int_{q_m}^{140} dq \frac{d\sigma^{Z\gamma}}{dq}$ is plotted ($d\sigma^{Z\gamma}$ is the cross-section for the process $p\bar{p} \to Z(\gamma)X \to e^+e^-X$).

The theoretical errors quoted in table 2 take neither the Λ^{QCD} and parton density ambiguity nor the phase space truncation with respect to q into account; they are rough estimates based on the following list of possible sources of uncertainties :

1. The numerical integration procedure ($\pm 1\%$).
2. The ambiguity of the top mass value ($\pm 1\%$ on σ_{tot}^{W}).
3. The contribution of $O(\alpha_s^2)$ terms to the perturbative tail of the q_T distribution (between +0.5% and +1.5% at $\sqrt{s}$=0.63 TeV, between +1% and +3% at $\sqrt{s}$=1.8 TeV). This evaluation is based on the work of Arnold and Reno [5] and on the fact that the contribution of the q_T tail ($q_T > 20\,\text{GeV}$) to σ_{tot} is about 5% at 0.63 TeV and about 10% at 1.8 TeV.
4. The contribution of terms which are beyond the leading double logarithmic approximation — *i.e.* $O[\alpha^n(q_T^2)\ln^{2n-2}(q^2/q_T^2)]$ terms — ($\pm 4\%$ at 0.63 TeV, $\pm 2\%$ at 1.8 TeV); this *rough* estimate is based on a study of the Kodaira-Trentadue [27] nonleading contribution performed by Altarelli et al. [8]; these

[6] Results from this reference are obtained with the same parton densities set as ours; on the other hand, only on shell W and Z are considered and a different choice of weak parameters is used ($M_W = 81.8\,\text{GeV}$, $M_Z = 92.6\,\text{GeV}$). However, in this context, this choice is not crucial, because the *normalized* distribution $\frac{dR}{dq_T^2}$ is poorly sensitive to it.

authors claimed that the Kodaira-Trentadue correction produces an effect of the same magnitude as the one produced by changing Λ by a factor of about 1.5.

5. The contribution of diagrams with initial photon Bremstrahlung (between +0.5% and +1%); this number is obtained by translating the contribution of initial *gluon* Bremstrahlung to the photon case.

6. Other higher order corrections. Even though we have no estimates for this contribution, we would be surprised if it is larger than a few per cent.

7. Other sources (< 1%); for instance, it is by now settled that initial interactions between active and spectator quarks do not affect σ_{tot} [28].

We have obtained our estimate for the relative error on the total cross-sections from the quadratic mean of the errors stated above, taken for granted that the items 3 and 5 lead to a shift of the overall relative error. For the error on the ratio R we only took items 1,2 and 7 into account.
For contact with previous work, we show the predictions of Arnold and Reno [5] for σ^Z_{tot} and $\sigma^{W^+}_{tot}$, calculated to *first* non-leading order and for the two scales q and $< q_T >$ in $O(\alpha_s)$ terms (see the footnote at page 51); in brackets are the results we have obtained with the same weak parameters as these authors:

at $\sqrt{s} = 0.63\,\text{TeV}$:	$\sigma^Z_{tot} = 60.5 - 87\,(65.7)\,\text{pB}$	$\sigma^{W^+}_{tot} = 308 - 418\,(329)\,\text{pB}$
at $\sqrt{s} = 1.8\,\text{TeV}$:	$\sigma^Z_{tot} = 206 - 208\,(207)\,\text{pB}$	$\sigma^{W^+}_{tot} = 1065 - 1050\,(1092)\,\text{pB}$

We end this chapter with the presentation of cross-sections projected on the leptonic variable l_T (transverse momentum of one of the final lepton) or m_T (transverse mass of the final lepton pair; $m_T^2 \doteq 2l_{1T}l_{2T}[1 - \cos\varphi(\vec{l}_{1T}, \vec{l}_{2T})]$ with the kinematics defined by eq.(1)). The figure 5 shows the shape of the Jacobian peak at fixed values of q_T; what is displayed is the quantity

$$R \doteq 10^2 \cdot \left(\left[\frac{d^2\sigma}{dq_T^2 dl_T} \right] / \left[\int_0^{100} dl_T \, \frac{d^2\sigma}{dq_T^2 dl_T} \right] \right)_{q_T \text{ fixed}}$$

The Jacobian peak $\frac{d\sigma}{dl_T}$ is displayed in figure 6 , while figure 8 shows the m_T distribution $\frac{d\sigma}{dm_T}$. All these curves are for $\sqrt{s} = 1.8\,\text{TeV}$ and are obtained from the fully differential cross-section integrated over the phase space region defined by $\sqrt{q^2} \in (70, 120)\,\text{GeV}$ for Z,γ production and by $\sqrt{q^2} \in (50, 140)\,\text{GeV}$ for W production. A common feature of these distributions is their high sensitivity to the weak vector boson mass, whilst their sensitivity to the choice of Λ^{QCD} and parton

densities is low; for this reason they form an important tool for the de termination of m_W and m_Z.

We compare our distributions $\frac{d\sigma}{dl_T}$ for virtual $W^{\pm}$ production for $m_W = 80\ GeV$ with direct calculations of the same quantity [1] , [10] in figures 7a and 7b:

In figure 7a our distribution is taken from ref. [11] (adapted to $m_W = 80\ GeV$). It is calculated for $\sqrt{s} = 630\ GeV$ using the methods described in this work. As structure functions the set DO1 from ref. [19] is used. The comparison is with the transverse electron distribution (Jacobian peak) calculated by Aurenche and Lindfors [1], for $\sqrt{s} = 540\ GeV$, $m_W = 80\ GeV$, using structure functions of ref. [29].

In figure 7b our distribution is calculated the same way as those displayed in figure 6 (adapterd to $m_W = 80\ GeV$) , with the structure function set DFLM g260 [18] . The common center of mass energy is $\sqrt{s} = 1.8\ TeV$. The comparison is with the Jacobian peak calculated by Baer and Reno [10] , for $m_W = 80\ GeV$, using set 1 of the EHLQ structure functions [30] .

We also emphasize that the highly non trivial structure shown in figure 5 could be used for a consistency check of the data analysis.

Finally, from CP invariance of the processes under consideration one derives the identities:

$$\frac{d\sigma^{W^+}}{dl_T(e^+)} = \frac{d\sigma^{W^-}}{dl_T(e^-)}\ ;\ \frac{d\sigma^{W^+}}{dl_T(\nu)} = \frac{d\sigma^{W^-}}{dl_T(\bar{\nu})}\ ;\ \frac{d\sigma^{Z}}{dl_T(e^+)} = \frac{d\sigma^{Z}}{dl_T(e^-)}$$
$$\frac{d\sigma^{W^+}}{dm_T} = \frac{d\sigma^{W^-}}{dm_T} \qquad (113)$$

Moreover, the relative difference $\left(\frac{d\sigma^W}{dl_T(\nu)} - \frac{d\sigma^W}{dl_T(e)}\right) / \frac{1}{2}\left(\frac{d\sigma^W}{dl_T(\nu)} + \frac{d\sigma^W}{dl_T(e)}\right)$ was calculated; its value is between -1% and 0% when l_T is smaller than 40 GeV and then linearly grows to reach nearly +9% for $l_T = 60$ GeV.

References

[1] K. Kajantie and P. Raitio, Nucl. Phys. B139 (1978) 72.
F. Halzen and P. M. Scott, Phys. Rev. D18 (1978) 337.
H. Fritzsch and P. Minkowski, Phys. Lett. 74B (1978) 384.
P. Aurenche and J. Lindfors, Nucl. Phys. B185 (1981) 274, 301.

[2] G. Altarelli and G. Parisi, Nucl. Phys. B126 (1977) 298.

[3] G. Altarelli, R. K. Ellis and G. Martinelli, Nucl. Phys. B143 (1978) 521, B146 (1978) 544, B157 (1979) 461.

[4] A. D. Martin, R. G. Roberts and W. J. Stirling, Phys. Rev. D37 (1988) 1161, Phys. Lett. 206B (1988) 327, CERN preprint CERN-TH.5112/88 (1988).

[5] P. B. Arnold and M. H. Reno, Nucl. Phys. B319 (1989) 37;
Erratum: Nucl. Phys. B330 (1990) 284.
P. B. Arnold, R. K. Ellis and M. H. Reno, Phys. Rev. D40 (1989) 912.
T. Matsuura, S. C. van der Marck and W. L. van Neerven, Phys. Lett. 211B (1988) 171.
E. Mirkes, J. G. Körner and G. A. Schuler, Complete $O(\alpha_s^2)$ Corrections to High p_T Polarized Gauge Boson (W, Z, γ^*) Production at Hadron Colliders, DESY preprint in preparation.

[6] Yu. L. Dokshitzer, D. I. Dyakonov and S. I. Troyan, Phys. Rep. C58 (1980) 269,
and references cited therein.

[7] J. C. Collins and D. E. Soper, Nucl. Phys. B193 (1981) 381, B194 (1982) 445, B197 (1982) 446.
S. C. Chao, D. E. Soper and J. C. Collins, Nucl. Phys. B214 (1983) 513.

[8] G. Altarelli, R. K. Ellis, M. Greco and G. Martinelli, Nucl. Phys. B246 (1984) 12.

[9] G. Altarelli, R. K. Ellis and G. Martinelli, Z. Phys. C27 (1985) 617.

[10] H. Baer and M. H. Reno, $O(\alpha_s)$ Corrections to Observables from $p\bar{p} \rightarrow W^+ X \rightarrow e^+ \nu X$, Florida State University preprint, FSU-HEP-901030 (1990).

[11] C. Greub and P. Minkowski in Proc. 1. Int, Symposium on The Fourth Family of Quarks and Leptons, New York Academy of Science, Vol. 518, N. Y. 1987, pp. 50 - 74.

[12] C. Greub, Helv. Phys. Acta 64 (1991) 61.

[13] V. V. Sudakov, Sov. Phys. JETP 3 (1956) 65.

[14] P. Minkowski, Phys. Lett. 139B (1984) 298.

[15] C. Greub, Calculation of lepton spectra from W production at the $Sp\bar{p}S$ collider, Univ. of Bern thesis 1989, unpublished.

[16] J. M. Bettems, Inclusive Lepton Pair Production through Virtual W,Z and γ Gauge Bosons in Proton-Antiproton Collisions at $Sp\bar{p}S$ and Tevatron Energies, Univ. of Bern thesis 1991, unpublished.

[17] J.M. Bettems, C. Greub and P. Minkowski, Inclusive Lepton Pair Production through Virtual W,Z and γ Gauge Bosons in Proton-Antiproton Collisions, Bern University preprint, BUTP-90/13 (extended version) , unpublished.

[18] M. Diemoz, F. Ferroni, E. Longo and G. Martinelli, Z. Phys. C39 (1988) 21.

[19] D. W. Duke and J. F. Owens, Phys. Rev. D30 (1984) 49.

[20] M. Glück, E. Hoffmann and E. Reya, Z. Phys. C13 (1982) 119.

[21] W. Hollik, CERN preprint CERN-TH.5661/90 (1990).

[22] G. Parisi and R. Petronzio, Nucl. Phys. B154 (1979) 427.

[23] F.A. Berends et al., Z Physics at LEP1, CERN 89-08 (1989), Vol. 1, p. 89.

[24] G. Burgers et al., *in* Ref. [23], Vol. 1, p. 55.

[25] UA2 Collaboration, J. Alitti et al., CERN preprint CERN-EP/90-20, Phys. Lett. 141B (1990) 150.

[26] CDF Collaboration: results presented by H. Grassmann at 'Les rencontres de physique de la valée d'Aoste', La Thuile, March 1990, and F. Abe et al. , Phys. Rev. Lett. 62 (1989) 1005..

[27] J. Kodaira and L. Trentadue, Phys. Lett. 112B (1982) 66, 123B (1983) 335.

[28] W.W. Lindsay, D.A. Ross and C.T. Sachrajda, Nucl. Phys. B214 (1983) 61.

[29] R. Baier, J. Engels and B. Petersson, Z. Phys. C2 (1979) 265, Z. Phys. C6 (1980) 309.

[30] E. Eichten, I. Hinchliffe, K. Lane and C. Quigg, Rev. Mod. Phys. 56 (1984) 579.

QCD running coupling constant	leading order form [from G.Altarelli et al. [8]]
Parton densities	3 parametrization sets from M.Diemoz et al. [18] (next-to-leading corrections included): g160 with $\Lambda = 160\,\text{MeV}$ ($\rightarrow \alpha_s(M_Z^2) = 0.107$) g260 with $\Lambda = 260\,\text{MeV}$ ($\rightarrow \alpha_s(M_Z^2) = 0.115$) g360 with $\Lambda = 360\,\text{MeV}$ ($\rightarrow \alpha_s(M_Z^2) = 0.122$) where Λ stands for $\Lambda_{4flavors,\overline{MS}}$ These sets will be refered as DFLM g160,...
Scale in pure perturbative terms	q_T
Switch from resummed to pure perturbative q_T-distribution	$q_T^{lim} = 20\,\text{GeV}$ for $\sqrt{s} = 630\,\text{GeV}$ $q_T^{lim} = 14\,\text{GeV}$ for $\sqrt{s} = 1.8\,\text{TeV}$
Parton active flavors	for Z production: u,d,s,c,b for W production: u,d,s,c
Electroweak parameters: Kobayashi-Maskawa matrix el. Weinberg angle Vector bosons masses and widths	$\lvert V_{ud}\rvert = 0.9755$, $\lvert V_{us}\rvert = \lvert V_{cd}\rvert = 0.22$, $\lvert V_{cs}\rvert = 0.9743$ $\lvert V_{ub}\rvert = \lvert V_{cb}\rvert = \lvert V_{td}\rvert = \lvert V_{ts}\rvert = 0$ as defined in [21]: $\sin^2\theta_W \doteq \bar{s}_W^2 = 0.231$ † $m_Z = 91.16\,\text{GeV}$, $\Gamma_Z = 2.49\,\text{GeV}$ † $m_W = 80.2\,\text{GeV}$ † , $\Gamma_W = 2.08\,\text{GeV}$ † † $m_W, \Gamma_W, \Gamma_Z, \sin^2\theta_W$ values are *calculated* from $\alpha, G_F, m_Z, m_t = 150\,\text{GeV}, m_H = 100\,\text{GeV}$ (refer to the text for a full discussion).

Table 1: Summary of the input parameters which, unless stated otherwise, are used in calculating our numerical results.

	σ_{tot}^Z [pb]	$\sigma_{tot}^{W^+} + \sigma_{tot}^{W^-}$ [pb]	$R = (\sigma_{tot}^{W^+} + \sigma_{tot}^{W^-}) \,/\, \sigma_{tot}^Z$
$\sqrt{s} = 630\,\text{GeV}$			
theory:			
DFLM g160	$67.6^{+4.4}_{-2.4}$	695^{+45}_{-24}	10.3 ± 0.3
DFLM g260	$65.7^{+4.3}_{-2.3}$	679^{+44}_{-24}	10.3 ± 0.3
DFLM g360	$63.8^{+4.2}_{-2.2}$	661^{+43}_{-23}	10.4 ± 0.3
UA2 result [25]	70.4 ± 6.8	660 ± 40	9.38 ± 0.84
$\sqrt{s} = 1.8\,\text{TeV}$			
theory:			
DFLM g160	202^{+10}_{-2}	2184^{+110}_{-22}	10.8 ± 0.3
DFLM g260	205^{+10}_{-2}	2226^{+110}_{-22}	10.9 ± 0.3
DFLM g360	205^{+10}_{-2}	2236^{+110}_{-22}	10.9 ± 0.3
CDF prel. result [26]	197 ± 34	2060 ± 340	10.5 ± 0.7

Table 2: Total cross-sections for the inclusive reactions $p\bar{p} \rightarrow W^{\pm}X \rightarrow e^{\pm} \overset{(-)}{\nu} X$ ($\sigma_{tot}^{W^+}, \sigma_{tot}^{W^-}$) and $p\bar{p} \rightarrow ZX \rightarrow e^+e^-X$ (σ_{tot}^Z), for $p\bar{p}$ collisions at 0.63 TeV and 1.8 TeV, calculated over the restricted phase space $\sqrt{q^2} \in (50, 140)\,\text{GeV}$ and with three different sets of parton densities (DFLM g160, g260, g360). The corresponding experimental results are reported; the quoted errors on these latter values result from the quadratic mean of statistical and systematic errors.

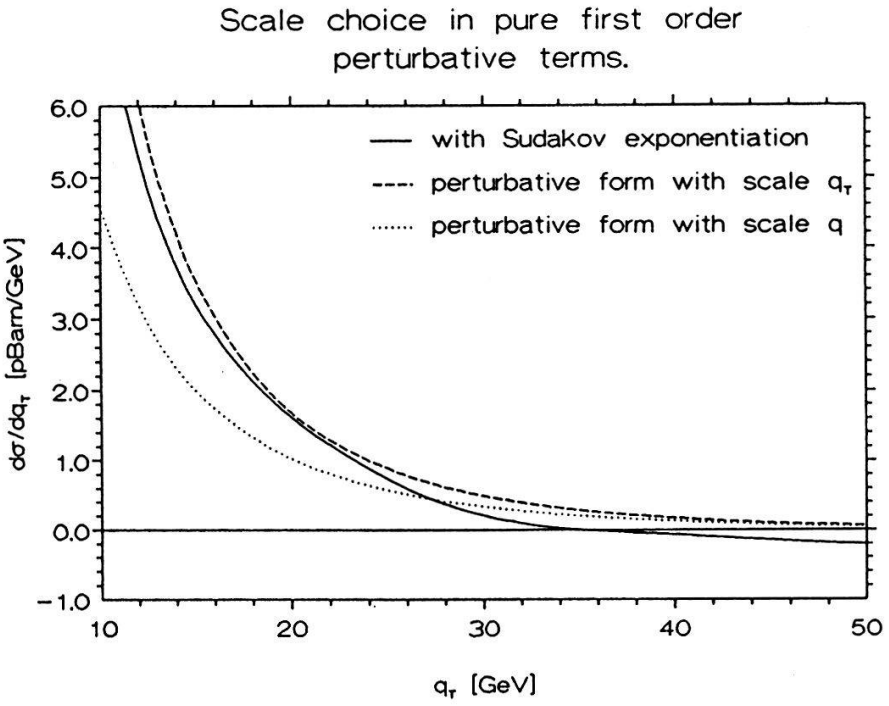

Figure 1: The transition region between the expression of $\frac{d\sigma}{dq_T}$ obtained by resummation of the soft gluons (Sudakov exponentiation) and the $O(\alpha_s)$ perturbative form, for two scale choices in the latter distribution. The plotted quantities are calculated for $p\bar{p} \to W^- X \to e^- \bar{\nu} X$ at $\sqrt{s} = 630\,\text{GeV}$ with the set DFLM g260 of parton densities (described in section 3). Similar curves can be drawn for Z production and at 1.8 TeV.

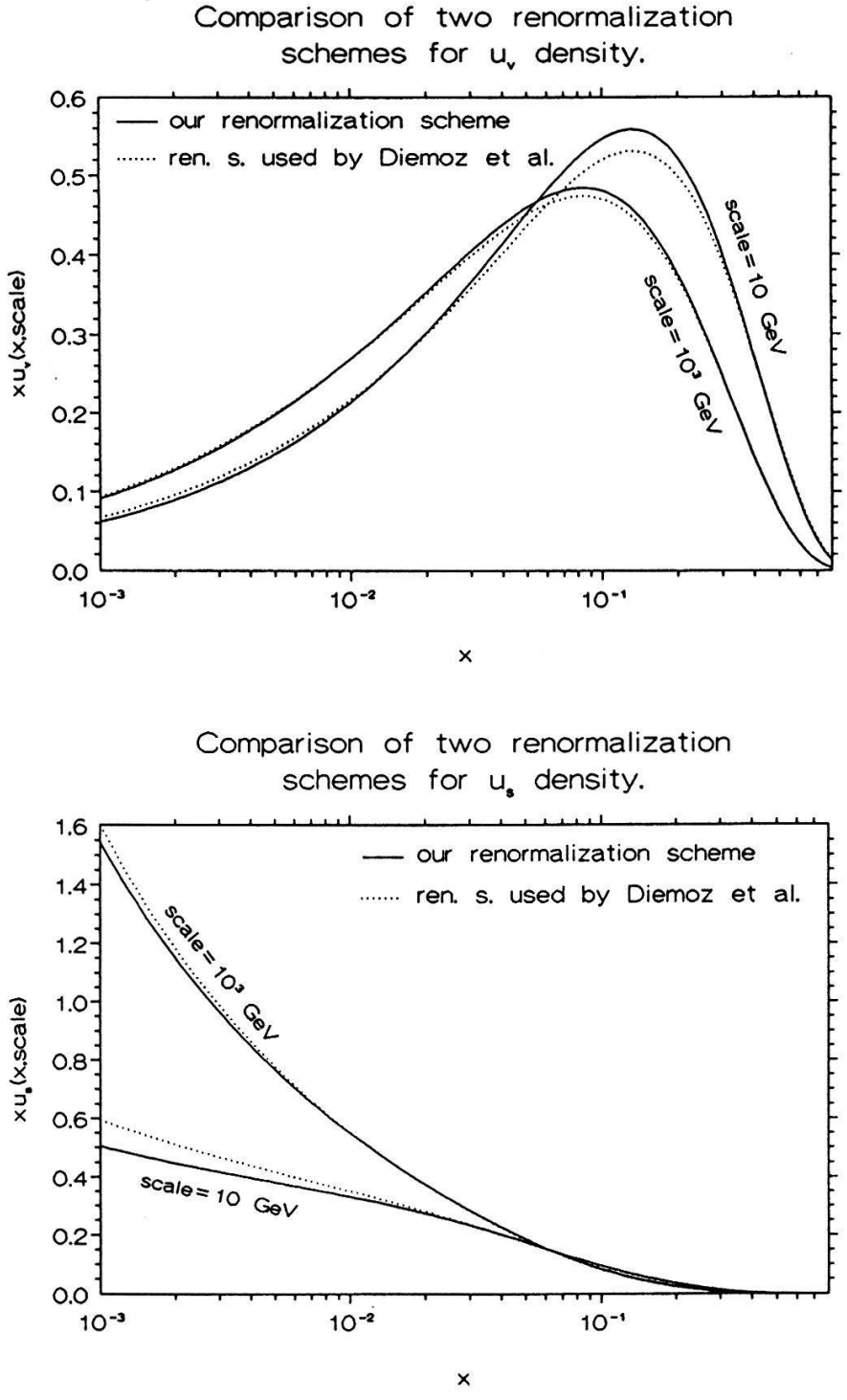

Figure 2: Comparison of two regularization schemes for the definition of parton densities. We show the up valence (u_v) and the up sea (u_s) densities (from DFLM g260) evaluated at scales of 10 GeV and 10^3 GeV.

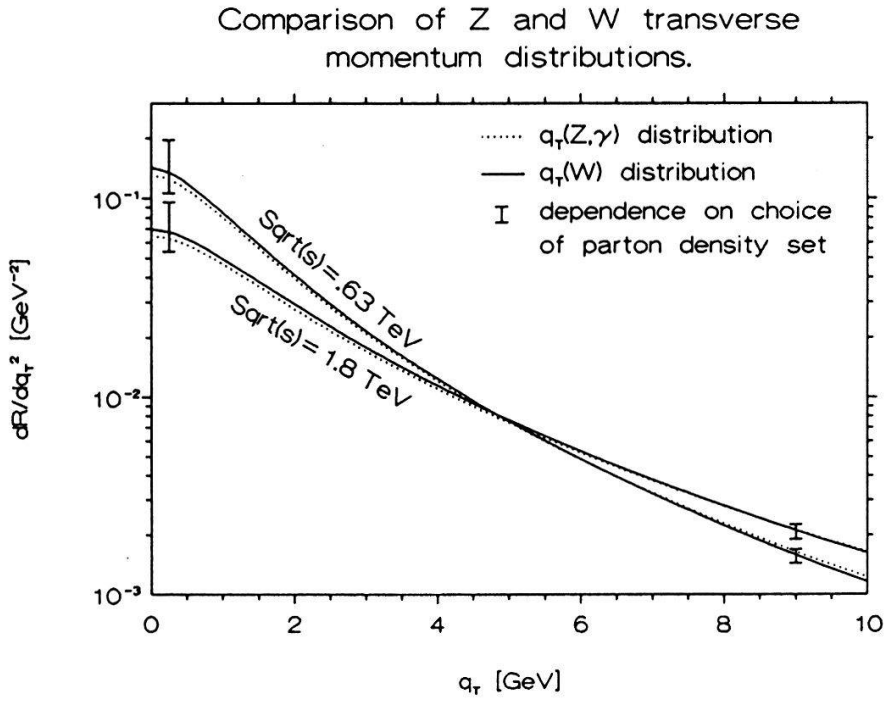

Figure 3a: This figure shows the normalized distribution

$$\frac{dR}{dq_T^2} \doteq \left(\int_0^{100\ GeV^2} dq_T^2 \frac{d\sigma}{dq_T^2}\right)^{-1} \cdot \left(\frac{d\sigma}{dq_T^2}\right)$$

for the transverse momentum squared of the vector boson produced in the reaction $p\bar{p} \to Z(\gamma)X \to e^+e^-X$ or $p\bar{p} \to W^\pm X \to e^\pm \overset{(-)}{\nu} X$ at $\sqrt{s} = .63$ TeV and 1.8 TeV. The set DFLM g260 of parton densities is used. The distributions for $Z(\gamma)$ are obtained by integration over the restricted phase space $\sqrt{q^2} \in (70, 120)$ GeV. The dependence on the choice of the parton density set shown in this figure is evaluated by using the three sets DFLM g160, g260 and g360.

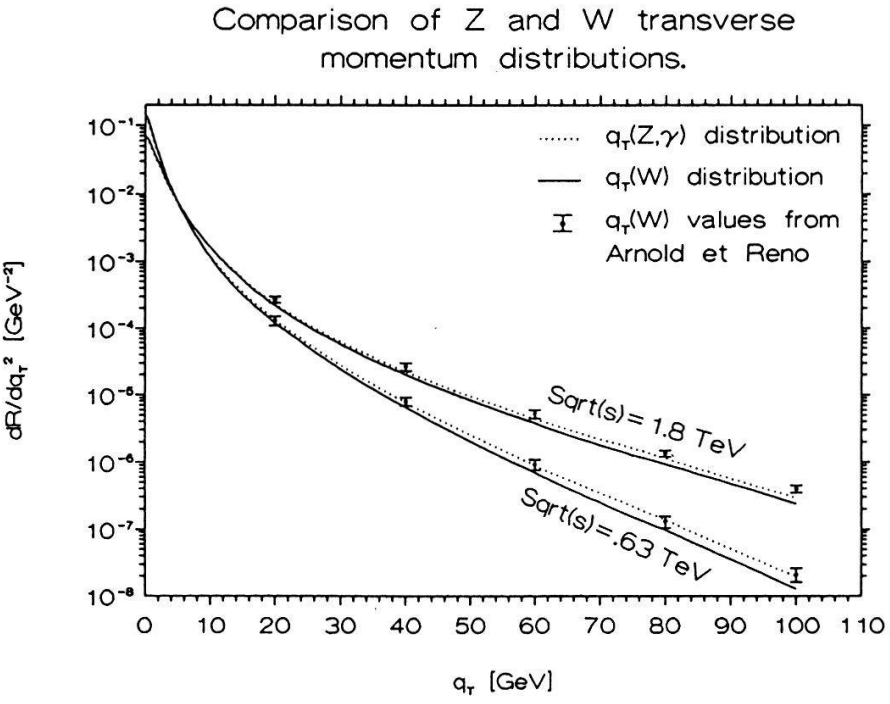

Figure 3b: Same as the figure 3a, but for the displayed points which give the values of $\frac{dR}{dq_T^2}$, for W production, obtained from the $O(\alpha_s^2)$ perturbative calculation performed by Arnold and Reno [5]; the error bars on these latter values include the effects of scale and Λ^{QCD} choice.

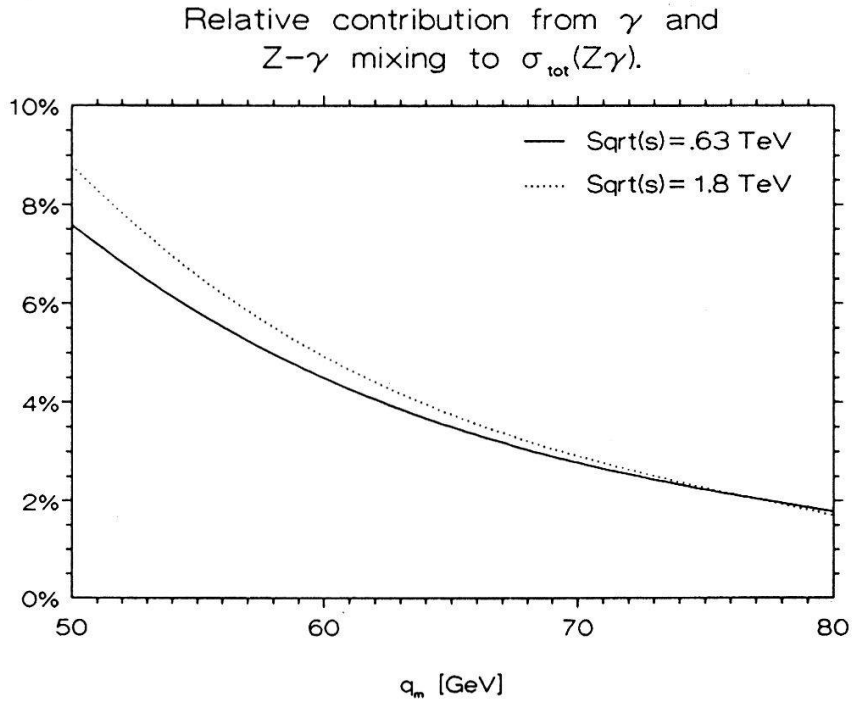

Figure 4: The relative contribution r from γ exchange and $Z\gamma$ mixing to the quantity $\int_{q_m}^{140\ GeV} dq\, \frac{d\sigma}{dq}(p\bar{p} \to Z(\gamma)X \to e^+e^-X)$ is plotted versus q_m.

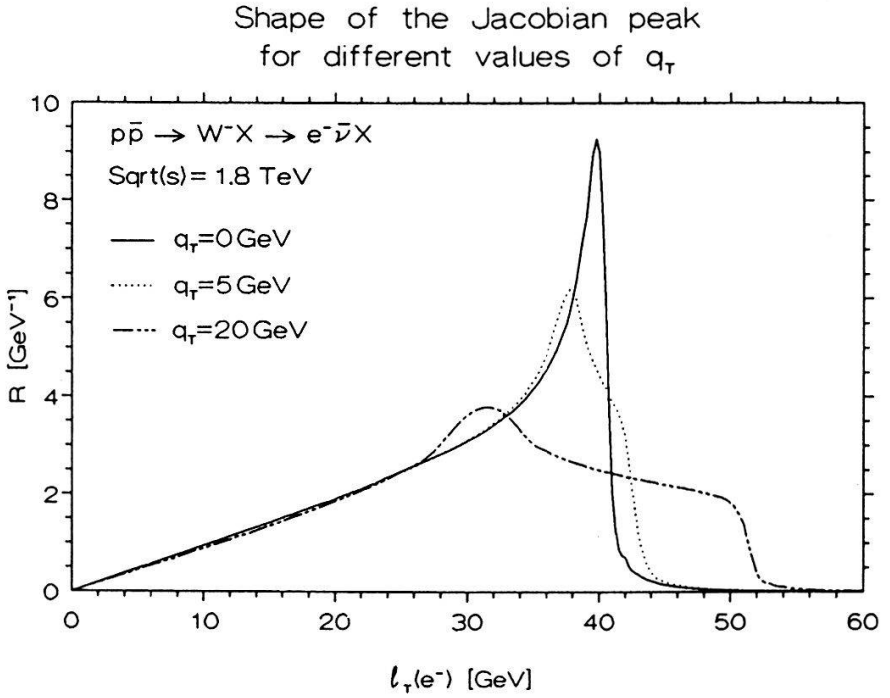

Figure 5: The shape of the Jacobian peak obtained at fixed values of q_T

$$R \doteq 10^2 \cdot \left(\left[\frac{d^2\sigma}{dq_T^2 dl_T} \right] / \left[\int_0^{100\ GeV} dl_T \frac{d^2\sigma}{dq_T^2 dl_T} \right] \right)_{q_T \text{ fixed}}$$

is plotted versus l_T (transverse momentum of the electron). The set DFLM g260 is used and $(d^2\sigma/dq_T^2 dl_T)$ is obtained by integration over the restricted phase space $\sqrt{q^2} \in (50, 140)$ GeV.

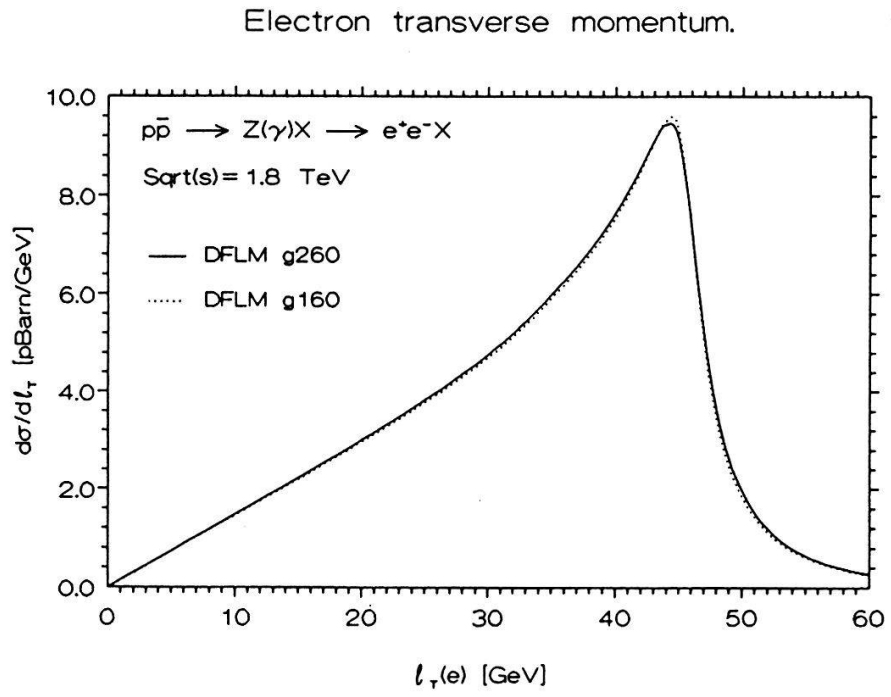

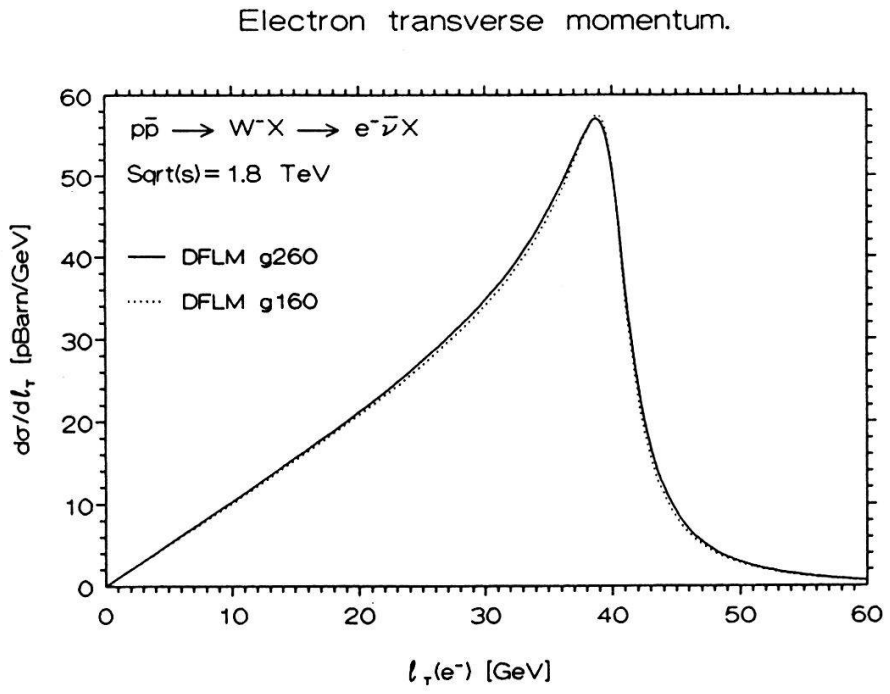

Figure 6: The Jacobian peak, $\frac{d\sigma}{dl_T}$, calculated for e^+e^- and $e^-\bar{\nu}$ production at $\sqrt{s} = 1.8\,\text{TeV}$ (l_T stands for the transverse momentum of the electron). The distributions for e^+e^- production are obtained by integration over the phase space region $\sqrt{q^2} \in (70, 120)\,\text{GeV}$, whilst the distributions for $e^-\bar{\nu}$ are obtained with $\sqrt{q^2} \in (50, 140)\,\text{GeV}$.

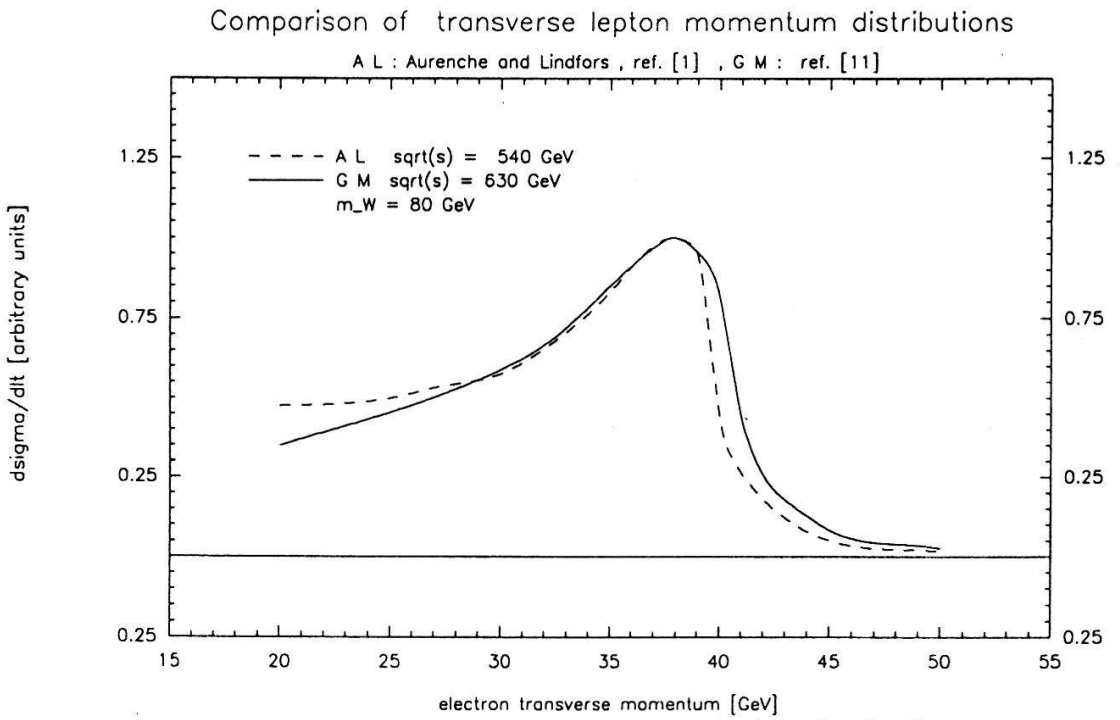

Figure 7a: Comparison of the Jacobian peak for virtual $W^{\pm}$ production for $m_W = 80\ GeV$, in ref. [11] , at $\sqrt{s} = 630\,\text{GeV}$, using the structure functions of Duke and Owens (set 1) [19] , with the calculation of the same quantity by Aurenche and Lindfors [1] at $\sqrt{s} = 540\,\text{GeV}$, with the structure functions of ref. [29].

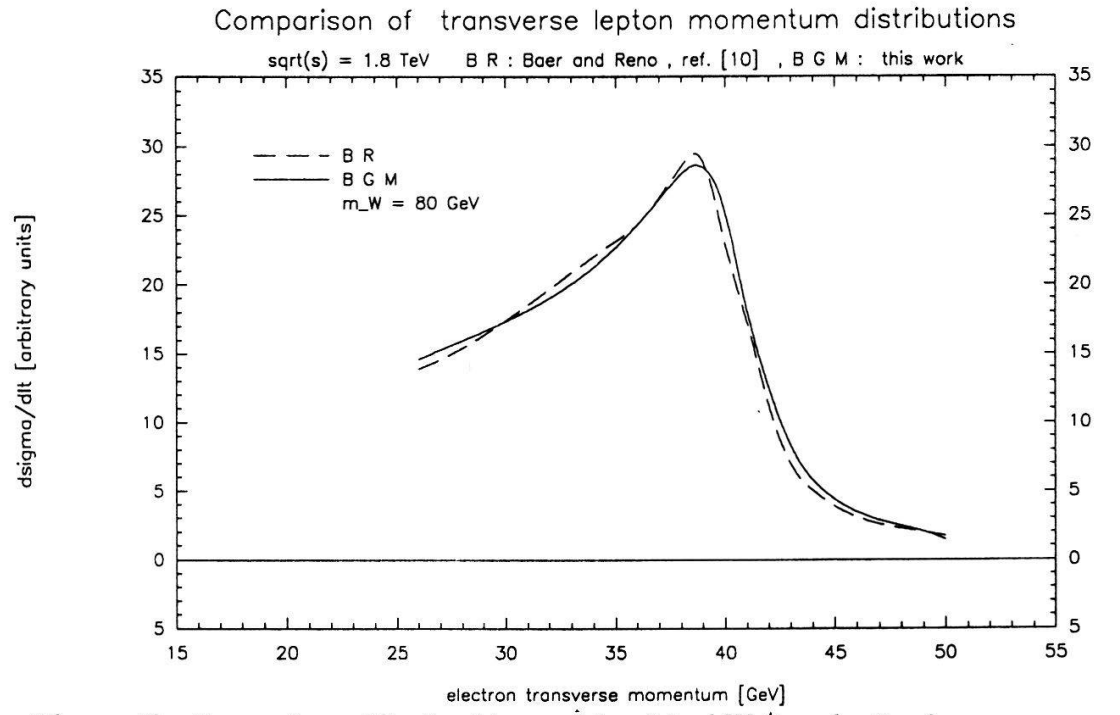

Figure 7b: Comparison of the Jacobian peak for virtual $W^{\pm}$ production for $m_W = 80\ GeV$, at $\sqrt{s} = 1.8\,\text{TeV}$ in this work , using the structure functions DFLM g260 , with the calculation of the same quantity by Baer and Reno [10], with structure functions of ref. [30].

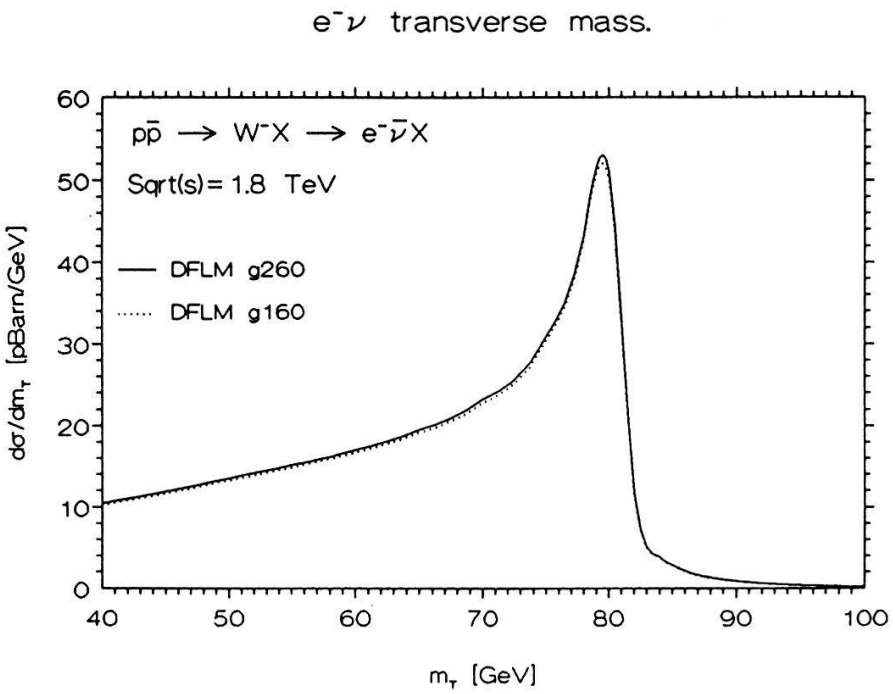

Figure 8: The distributions $\frac{d\sigma}{dm_T}$, where m_T stands for the transverse mass of the produced leptons pair, calculated for e^+e^- and $e^-\bar{\nu}$ production at $\sqrt{s} = 1.8\,\text{TeV}$ with the same phase space restrictions as those quoted in the caption of the figure 6.